Self-piercing riveting of dissimilar carbon fiber-reinforced composites and aluminum alloy sheets: state-of-the-art achievements

Liang Ying[1,2] · Quanyi Dong[2] · Tianhan Gao[2] · Minghua Dai[1] · Ping Hu[2]

Abstract

Lightweight design of the vehicle is critical in reducing carbon emissions and energy consumption. In recent decades, high-performance carbon fiber–reinforced plastic (CFRP) composites, which are the most direct and effective choice for lightweight designs, are broadly applied in the vehicle industry to meet both strength and lightweight requirements. However, among many reasons for car body manufacturing, the higher price of composite is one of the limitations for its application, so the utilization of hybrid composite materials and metallic materials is widely adopted together in guaranteeing the economy of vehicle development and manufacturing. Aiming at the hybrid metal-composite multi-layer joint combination requirement, how to implement a valid connection has become a complex challenge. Currently, the more popular mechanical join approach is using self-piercing riveting (SPR) technology. This paper summarizes the state-of-the-art achievements in the aforementioned research field to connect hybrid composites and metallic materials especially by using SPR methods, which involve the process, the joinability, the mechanical behavior of joints, and the corresponding FE modeling methods. This paper also provides a detailed discussion of self-piercing riveting from a relatively comprehensive point of view to provide perspectives for subsequent in-depth research.

Keywords Vehicle lightweight design · Hybrid metal-composite joint · Self-piercing riveting · Numerical simulation

1 Introduction

Nowadays, the underlying lightweight requirement conduces to the reduction of fuel consumption and environmental emission in the vehicle industry. The typical strategies involving structure optimization, process revolutionary and material innovation have been widely considered as three effective lightweight pathways, as shown in Fig. 1. One of the most direct and effective methods is the utilization of aluminum alloy, which is particularly prominent in the area of automotive lightweight with its high strength, corrosion resistance, and low plasticity characteristics. Specifically, ultra-high-strength aluminum alloy materials have begun to be applied in automobile body-in-white manufacturing, which becomes an academic frontier [1, 2]. In addition, carbon fiber–reinforced plastic (CFRP) composites have also been increasingly focused on the relevant research, including the investigation of the CFRP manufacturing process, the study aiming at the anisotropic fiber damage model, and exploration of related hybrid Al-CFRP connection methods [3–8], have been flourishing.

The application of advanced composites in the automobile industry is described in Elmarakbi [9], where the overall structure and collision resistance are analyzed. The main content shows that when composites are applied to vehicles, they can greatly reduce the weight of a vehicle while increasing its strength. Kim et al. [10] investigated the performance of square hollow cross-section (SHS) beams made of CFRP and aluminum alloy composite under dynamic axial crushing load when used on energy-absorbing boxes. The team also conducted low-speed impact tests using RCAR rules in five different layer sequences and two different laminated thicknesses. Gao et al. [11] utilized carbon fiber–reinforced composite materials and epoxy substrate materials to conduct a series of experimental tests

✉ Liang Ying
  yingliang@dlut.edu.cn

1 School of Mechanical Engineering, Dalian University of Technology, Linggong Road 2#Liaoning Province, Dalian 116024, People's Republic of China

2 School of Automotive Engineering, Dalian University of Technology, Dalian 116024, People's Republic of China
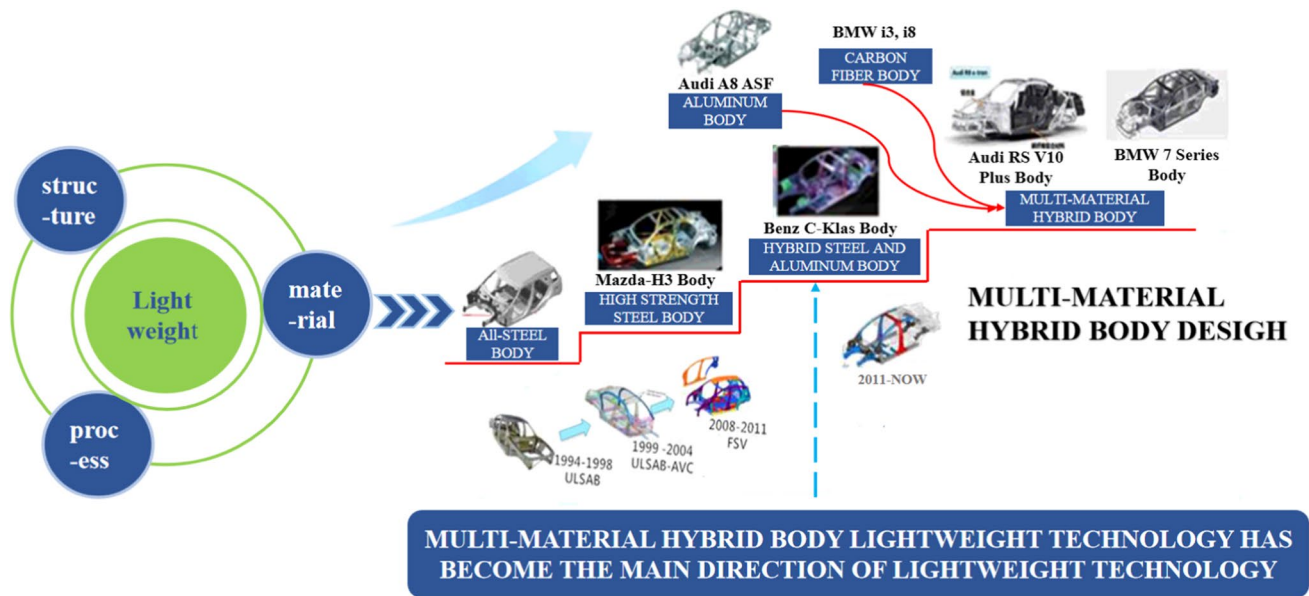
Fig. 1 Development tendency of vehicles light-weighting in recent years

carried out on the hood of an SUV hybrid model. The results of their various operating tests evidence that the performance improvement of CFRP hood compared to steel hood is more than 10% and the weight is reduced by 45.56%. Zang et al. [12] put forward the structural/material integrated design for the structural layout and laminate layer's optimization of the automotive composite anti-collision beam, which increased the strength of the anti-collision beam structure by 81.41%. All the above evidence shows that CFRP can meet the requirements of automobile lightweight well. Nevertheless, since carbon fiber composites are expensive and have a limited range of use in some low- and medium-end vehicles, engineers often introduced composites combined with metals in most cases [13, 14].

Mechanical connection based on the principle of plastic deformation can improve accuracy, reliability, and environmental safety; thus, it has been widely accepted in the vehicle manufacturing industry. However, it is a prevalent challenge to be effectively connected to heterogeneous metallic and composite materials. In particular, traditional resistance spot welding can generate a thick oxide film on the surface of the aluminum sheets, which leads to poor connection strength and quality. Therefore, developing a reliable and efficient join technology for connecting hybrid metal-composite material parts is necessary to avoid surface treatment of sheets and further save time and economic costs. For this reason, Mori et al. [15] outlined several popular ways to join different materials, including bonding, condensation welding, frictional stirring welding, self-piercing riveting, and clinching. Zheng et al. [16] studied the mechanism of damage, the failure process, and the failure mode of aging

areas when using the boding joints of CFRP and aluminum alloys after wet and thermal degradation. They further discussed the application of bonding technology in the automotive industry. Ren et al. [17] connected the Al5052 and CFRP through coaxial resistance spot welding. They studied the cross-sectional and mechanical characteristics of their single-lap joints. Kumar et al. [18] studied the effect of plasticity on the strength of joints in the shearing structure by clinching and concluded that plasticity is the main factor.

Although the academic pioneers have put a lot of effort into different connection approaches, considering the cost, efficiency, and practicality, no doubt that self-piercing riveting (SPR) has become a vital joint technology for automobile metal sheet connection technique due to its advantages of no need for pre-punching and being free from the limitations of the type and number of sheet layers. Generally, the mechanical behavior and failure mode of SPR joints is determined by the mechanical interlocking structure formed through the plastic deformation between the rivet leg and the stacked multi-layer sheets. The interlock factors include the combination of sheets, sheet geometrical parameters including the sheet thickness and the rivets/die shape geometries, and the mechanical properties of the materials such as flow stress, plasticity, strength, etc. Nevertheless, for advanced high-strength metal and non-metallic materials, the conventional SPR, as the preferred cold-forming fastening method, faces more challenges because it is a cold-forming connection method based on plastic deformation. This process is restricted to the limited formability of high-strength steels, aluminum alloys, and composites (e.g., DP980 steel, 7075-T6

aluminum alloys, CFRP/GFRP) at ambient temperature. In addition, because of multi-stacking, low ductility, and high strength issues, self-piercing riveting can also easily lead to fracture and weak interlock structure, etc.[19].

Therefore, inspired by the idea of thermoplastic deformation to reduce flow stress and the strength of substrate materials, some scholars recently developed a series of improved SPR methods by heating dies of sheets to control the flow stress of metals, thereby improving the connection performance of the classic SPR process. Compared with conventional self-piercing riveting processes at ambient temperature, most improved solutions, including local induction heating, laser-assisted heating, and flame heating, have been introduced into the conventional SPR process by pre-heating the connected sheet to a deformable range. For instance, Jackel et al. [20] introduced a sensor directly integrated into the ceramic die for heating connected sheets, which contributes to reducing the processing time and avoiding the use of riveting machine heating. The laser-assisted SPR (LSPR) technology for AZ31 magnesium alloy strips has been developed by Durandet et al. [21]. Crack-free riveting joints are realized when the strip temperature exceeds 200 degrees to meet various strength requirements. Zhuang et al. [22] developed a flame-assisted spring device for connecting ultra-high-strength steel plates and aluminum alloy plates.

However, controlling a uniform temperature field of multilayer sheets in a local riveting area is still a challenge for the aforementioned local heating methods. Furthermore, it is worth noting that local annealing and uneven temperature distribution can lead to residual thermal stress distribution, which can have a significant impact on the formation of cracks in the joints. Aim at the above problems, Ying et al. [23] proposed the improvement of the overall heating of the sheets to be riveted. They connected the high-strength AA7075-T6 aluminum alloy sheets after the overall heating evaluation of the best riveting temperature by self-piercing riveting pathways and significantly improved the joint quality of high-strength metallic materials. However, the above-modified thermal-SPR method has not been extended to the hybrid metal-composite joint issue yet.

In sum, aiming at the connection of hybrid heterogeneous metal-composite materials, various novel connection technologies have been developed in respective fields. In particular, self-piercing riveting is one of the best pathways to connect carbon fiber composites and aluminum alloys based on the principle of plastic deformation. The relevant investigations are a hot topic in recent decades. In this paper, a great amount of SPR studies associated with how to connect with carbon fiber composites and aluminum alloys is remarked reviewed from the five aspects of the process, the joint forming quality, the joint mechanical behavior, the joint corrosion failure, and the numerical modeling method to roundly provide orientation and guide for future in-depth research.

2 Methodology and equipment requirement of self-piercing riveting

2.1 Self-piercing riveting process

The self-piercing riveting process was first proposed by Fuhrmeister [24] in 1977 and has since developed into an important plastic connecting technology in automotive body sheet metal components. The greatest advantage of self-piercing riveting technology is that it avoids the pre-punching step of the traditional riveting process and is not limited to the type and number of layers of the sheets so that the connection of heterogeneous plates such as composite materials and metals can be realized. Over the past years, the connection of metal sheets based on the SPR process has been widely studied and tends to mature [15, 25–28]. However, the connection of heterogeneous sheets including composites and metals has only begun to gain focus from relevant scholars in recent years [6, 29–32].

The main process of the self-piercing riveting process, as shown in Fig. 2, can be divided into the following four key steps:

Sheet positioning. The pending riveting sheet is placed horizontally on the die of the self-piercing riveting machine and must ensure that the riveting area center point is coaxial with the punch of the self-piercing riveting machine.

Pressing edge to rivet. The blank holder first moves down and then clamps the sheets with the cooperation of a die by hydraulic pressure, which ensures that the sheets will not move in the riveting process. Afterward, the punch pushes the rivet down to penetrate the upper sheet and is stuck in the lower sheet. In this process, the rivet leg flares outward under the deformation resistance of the lower sheet and die, and the lower sheet flows plastically at the same time. This process forms a permanent mechanical interlock structure within the joint to achieve a reliable mechanical connection.

Pressure maintaining. After the riveting process is done, the oil pressure is maintained to let the punch stay at the limit position for 5–10 s so that the lower sheet under the punch pressure can fully flow to fill the entire die, thereby minimizing rebound deformation.

Unloading and punch releasing. After the above three steps are completed, the oil pressure is discharged, the punch and blank holder are pushed up, and the specimen is taken out to complete to entire riveting process.

2.2 Self-piercing riveting equipment

Based on the principle of the SPR process, a brief overview of the current self-piercing riveting connection research and corresponding equipment is introduced in this chapter. The

Fig. 2 Principle of the basic SPR process [33]

Clamping   Piercing   Flaring   Releasing
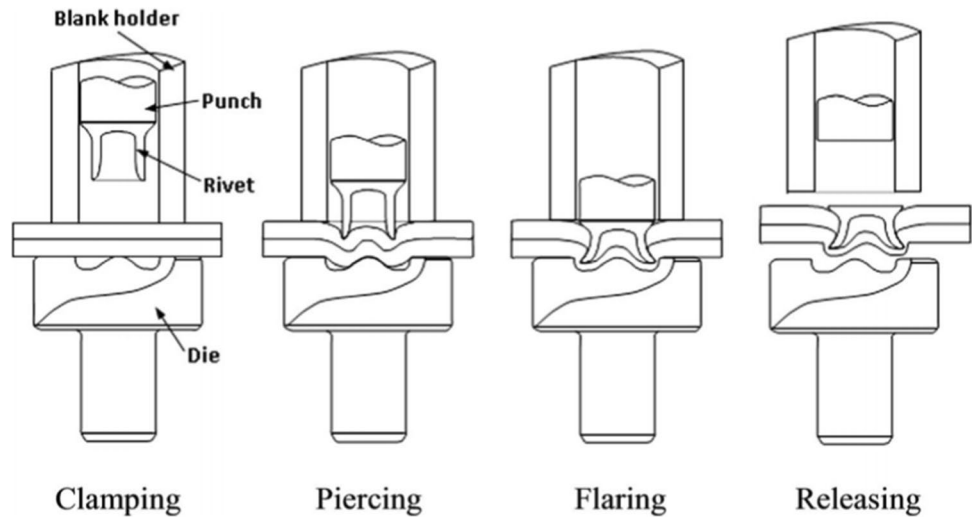
equipment used for self-piercing riveting connections mainly consists of different unit devices, the key unit of which is a C-frame with integration. As shown in Fig. 3, rivets are mounted on the rivet belt and transported to the riveting gun via a feeding system. So, the rivet setter is then worked, and the riveting process is completed through the manual/self-driven control unit to drive the power unit.

Currently, two typical SPR facilities are utilized to rivet homogeneous or heterogeneous materials in recent investigations. Ying et al. [23] used a hydraulic self-piercing riveting machine ZOT-5T (ZOT, Dongguan, China) to

investigate the feasibility of the thermal self-piercing riveting for AA7075-T6 alloys, which is connected to AA7075-T6 aluminum alloy sheets under quasi-static loading conditions, as shown in Fig. 4a. In contrast, the limitation of this equipment is that the corresponding units are not integrated to monitor forces and displacements during riveting. Therefore, it is impossible to get the process details when riveting into the plate directly. An improved version of SPR equipment for self-piercing riveting of aluminum and copper alloy heterogeneous metal sheets was reported in He's work [28], which was fabricated by the commercial Böllhoff. Co. Ltd. The window
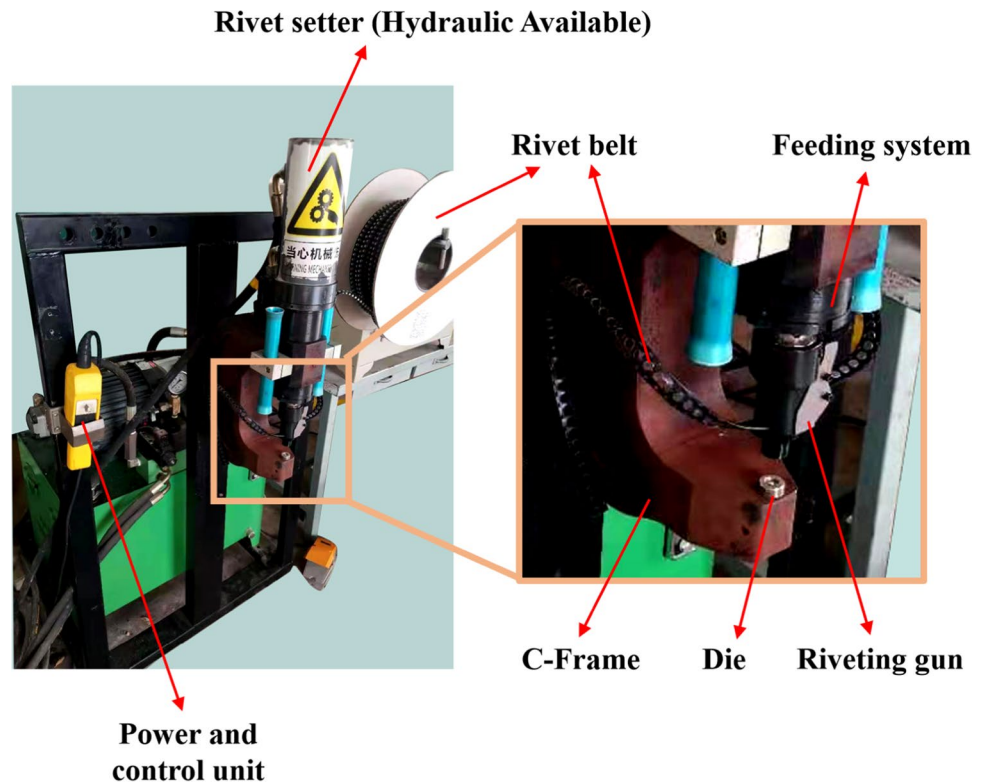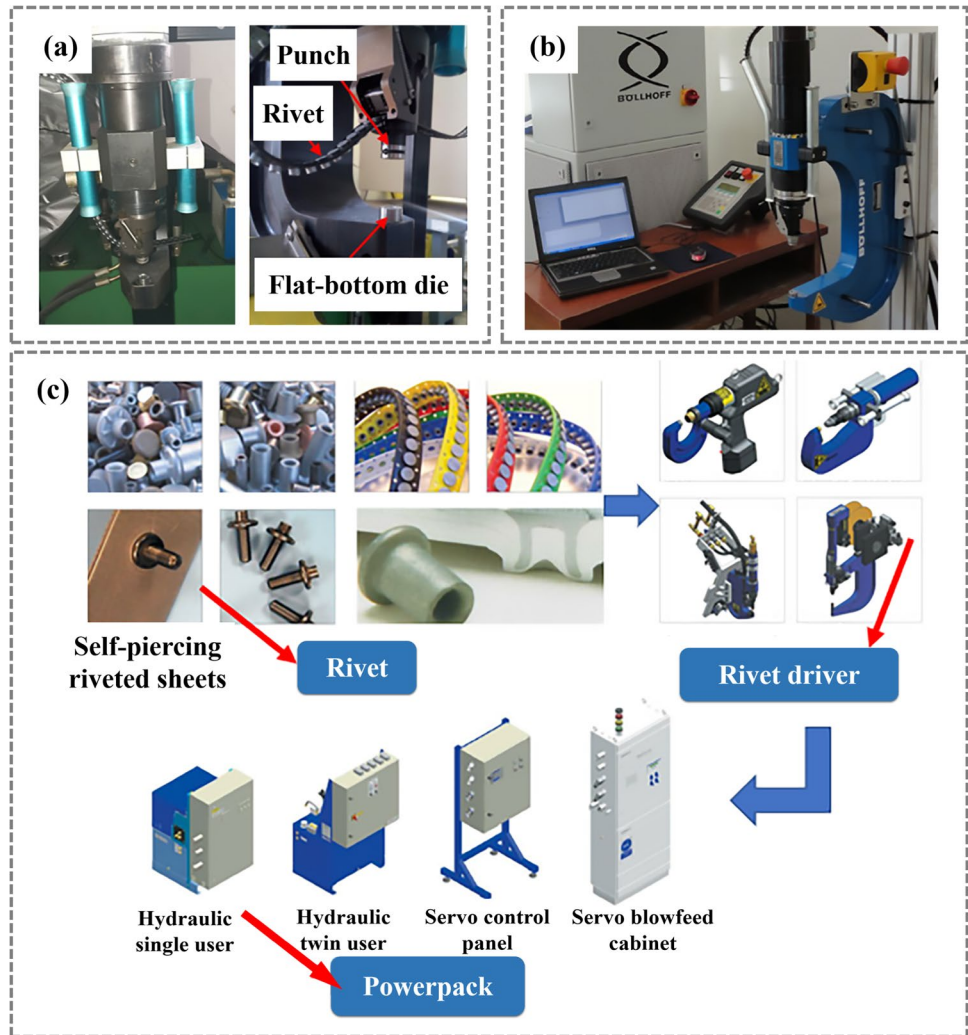
Fig. 3 Basic units of the SPR equipment

Fig. 4 **a** Traditional SPR equipment without integrated monitoring components [23]. **b** SPR equipment with integrated monitoring components [28]. **c** Advanced Henrob's SPR equipment [34]

monitoring system was integrated into this SPR device, as shown in Fig. 4b. It is capable of measuring the actual punch force and stroke in the riveting process through the force and position sensors. Then, the corresponding signal after amplification is then transmitted to the data acquisition system to generate the force–displacement curve. The whole process realizes the monitoring of the riveting process. Therefore, it is more convenient for scientific investigation under the allowed conditions. In addition, Henrob [34] has also developed a higher integrated account of electro-hydraulic servo SPR equipment including tailored rivets, C-frame rivet driver, and multiple electro-hydraulic servo control system, as shown in Fig. 4c. The detailed comparison of three various SPR facilities are shown in Table 1.

In sum, through a simple C-type frame structure, rivets can be automatically assembled through a riveted belt in current SPR facilities. The original self-piercing equipment can be redesigned and improved to suit specific research requirements and different technical requirements. Furthermore, due to the short assembly time, the C-type

Table 1 Comparison of various SPR facilities

References	Manufacturer	Riveting head structure	Power type	Force–displacement acquisition	Rivet die type
Ying et al. [23]	ZOT Automation Technology Co. China	C-frame	Hydraulic	No	DZ, FM
He et al. [28]	Böllhoff Co.Ltd, Germany	C-frame	Hydraulic	Yes	DZ, FM
Henrob [34]	Henrob, Co.Ltd, England	C-frame	Electro-hydraulic servo	No	Flexible, etc

riveting frame structures are widely used in the different automatic assembling SPR processes, and the modified SPR equipment is also multifarious.

3 Rivetability of the heterogeneous carbon fiber–reinforced plastic/metal joints

3.1 Methodology for evaluating the joint quality

As mentioned above, the SPR technology is not only unrestricted by the type of sheets but also behaves outstandingly in connecting heterogeneous sheets. Although this paper focuses on utilizing the SPR technology to connect composite materials and metallic sheets, in terms of the joint quality, the evaluation criterion of joint quality when using SPR to connect metal sheets is also critical in providing insights into the joining mechanisms. Therefore, this subsection broadly starts with the research on SPR connection technology [35–38], reviewing the evaluation methods of SPR joint quality, which also work with carbon fiber composite materials and aluminum alloys. These studies, through various aspects, including finite element methods, deep learning methods, and process routes, try to carry out a comprehensive and detailed analysis of the joint quality of SPR. However, the final landing point of all joint forming quality investigations is in the cross-profile morphology evaluation of joints. In one aspect of the macro-scope, whether the joint is cracked, fold, or eccentric should be considered. In the other aspect of the microscope, the analysis of the deformation through the cross-section of joints is essential.

In general, the joint morphology of their top and bottom surfaces is observed to evaluate the forming quality of SPR joints from a macro point of view. The joint quality is characterized by the deformation degree, fracture, and other aspects of these surfaces. Zhang et al. [30] studied the SPR connection of the PA6-based thermoplastic composite sheet and the 5754 aluminum alloy in recent years. In their study, the macroscope of SPR joints is characterized by cross-section and top–bottom surface to acquire a more comprehensive understanding of the deformation of the riveting process. Figure 5 shows the top and bottom surface macroscope, respectively. The joint quality is evaluated from the quality of the joint morphology. According to Fig. 5a, the bottom joint is significantly eccentric and the carbon fiber composite on the top surface of the joint cracked in Fig. 5e. These are the visual reflection of the fact that the joint does not meet the connection requirements in this case.

In contrast, advanced DIC (Digital Image Correlation) technology offers the possibility of higher precise and detailed morphology observation of SPR surface joints. For instance, Sadowski et al. [39] observed the riveted joint and its upper surface by DIC during the joint forming process.

Figure 6 (a1) shows the experimental method. Three-dimensional displacement distribution near the rivet during the riveting process can be easily acquired and then the principal strain state is estimated conveniently based on this method, as shown in Fig. 6 (a2). Suppose the DIC technology is appropriately applied to the riveting process, the deformation of the area near the rivet can be accurately observed in the riveting process.

Moreover, Ueda et al. [40] proposed an improved SPR technique to mechanically fix CFRP laminates, which consist of a rivet body and two flat washers. The two flat washers suppress the delamination of CFRP laminates at the riveting point. The forming quality of the joint is also characterized by macroscopic topography, as shown in Fig. 6 (b). Thus, the improvement of the joint can be observed in the forming quality.

Beyond that, serials of quantitative analysis of the microscopic cross section are also introduced to evaluate the joint quality of SPR other than the above macroscopic characterization. Specifically, a series of geometrical indicators are introduced to evaluate joint quality in recent investigations. It is essential to highlight the review conducted by Haque [41] on the quality of SPR connections that reflect the joint quality from a cross-sectional perspective. A sequence of indicators that quantitatively characterize the joints quality from the cross-section can be represented to be all included in Fig. 7. All elaborate cross-sectional parameters mentioned below are illustrated in this figure including the diameter of the leg before and after the deformation of the rivet, the thickness of the plate, the height of the rivet head, the biting edge of the rivet leg, etc.

One of the critical indicators to evaluate the joinability of the riveted joint is the leg flaring, which is the position of x in Fig. 7a. The size of the x value indicates the degree of interlock. The higher interlock value contributes to obtaining better performance of the entire joint. Not merely the interlock value, the head fit TS is also a critical measurement. The higher TS value leads to a minor degree of the rivet and upper plate combination, which indicates that the riveting connection is more unreliable. For example, Fig. 7b shows a cross-sectional morphology of riveting joints with different interlock values and head heights. In general, macroscopic observation is a convenient and efficient method for evaluating the quality of self-piercing riveting joints. It is used to directly observe the morphology of the joint after completing the connection process to affirm whether the joint is valid or the joint is eccentric and whether the fracture occurred at the sheets. If any invalid connection occurs, it can be directly determined that the joint connection has failed without the need for further analysis. As for microscopic measurement, it is necessary to cut the joint to obtain the cross-sectional morphology of the joint when no unqualified conditions are found in the macroscopic evaluation,

Fig. 5 Appearance of SPR joints for hybrid composites and metal sheets [30]. **a** PA6 on the top. **b** PA6 at the bottom for joints of PA6 and Al. **c** GFRP on the top. **d** GFRP at the bottom for joints of GFRP and Al. **e** CFRP on the top. **f** CFRP at the bottom for joints of CFRP and Al
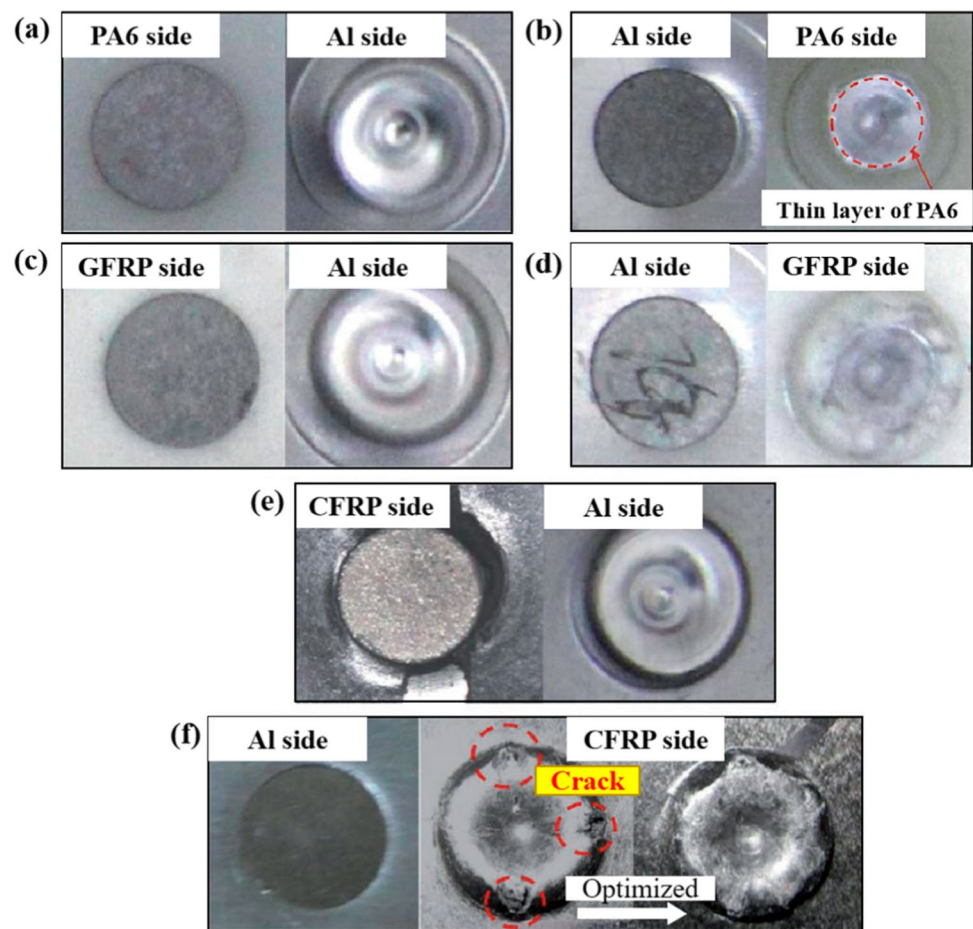
and then measure various indicators of the joint's medial surface through means such as electron microscopy. Currently, the leg diameter value x mentioned in Fig. 7a is often used for microscopic measurement of the joint's meridian plane. It reflects the interlocking structure formed by the rivet and bottom sheet, which directly reflects the strength of the joint. The larger the interlocking value x means the higher the strength of the joint. In addition, the remaining bottom thickness b, the effective length t_{eff} of the rivet at the bottom plate, and other indicators, as shown in Fig. 7a, can also be used as evaluation criteria for joint quality. After evaluating the joint quality through macroscopic observation and microscopic measurement, effective and reliable analysis results for self-piercing riveting can be obtained.

3.2 Technological factors of the self-piercing riveting process

Technological factors that affect the forming quality of heterogeneous SPR joints mainly include the length and sharpness of the rivet legs, the force and the rivet speed of punch, the blank holder force, the type of die, and the sheet materials, etc. As for the sheets, the influencing factors

mainly include the stacking order, the nature of the material (e.g., ductile or brittleness, etc.), and thickness, as classified in Fig. 8.

3.2.1 Influenced by the die, rivet, and punch

The joint forming quality above is also affected by the entire riveting process factors, of which the type of die, the diameter, length, and sharpness of the rivet legs, as well as the speed of punch, and the numerical magnitude of the force are all tightly associated. As for the type of die, two kinds of general dies are usually adopted, one is a flat bottom called FM type, and the other is the die with a raised center called DZ type, which are shown in Fig. 9a. In addition, three profiles of DZ dies for SPR are usually used in a recent investigation, as shown in Fig. 9b.

Mori et al. [42] studied the self-piercing riveting for joining ultra-high-strength steel and aluminum alloy sheets. They took into account that the deformation constraint effect decreased as the diameter of the die cavity increased. On the one hand, resulting in a decrease in the punch load, and may eventually be less than the load required for riveting. On the other hand, the punch force also decreased with the
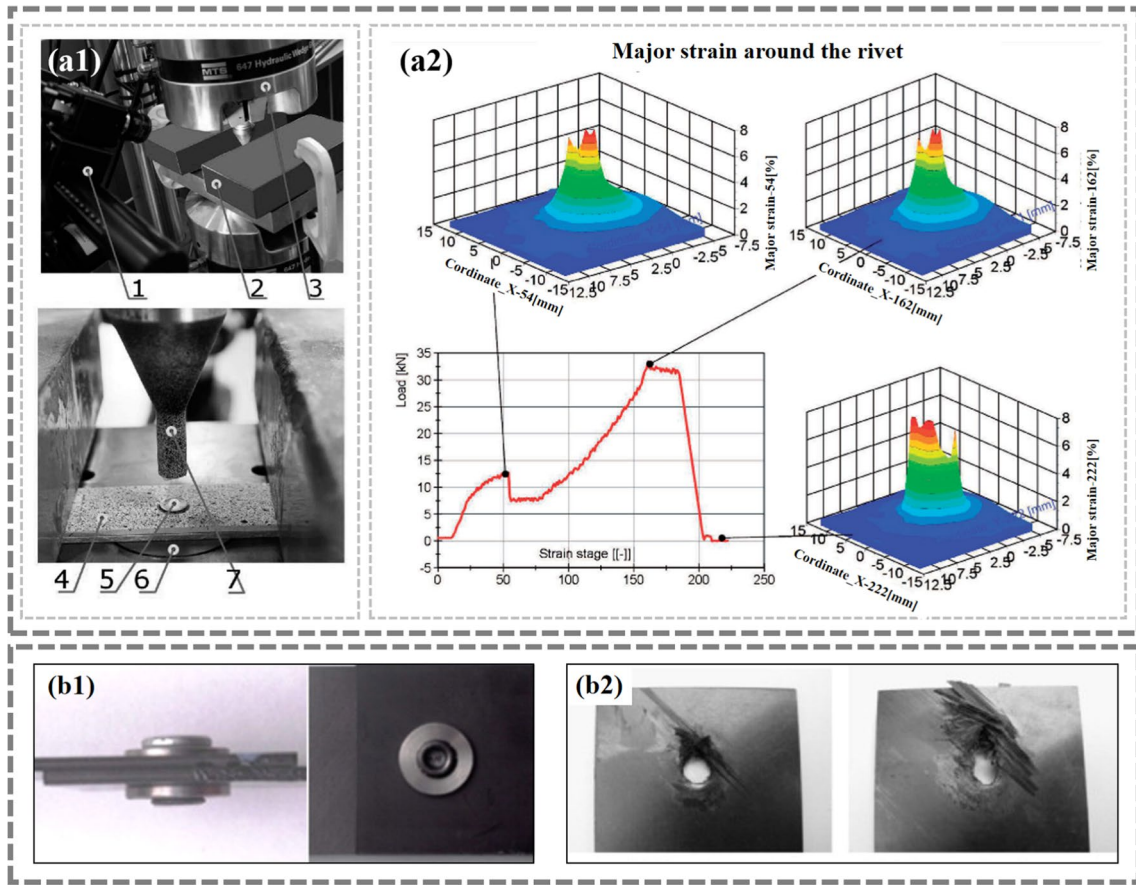
Fig. 6 (a1) DIC testing stand for piercing monitoring (1-DIC sensor, 2-blank holders, 3-MTS servo-hydraulic machine, 4-top aluminum2024 strip, 5-C-SKR rivet, 6-die, 7-punch) [39]. (a2) Deformation zone in 3D analysis the major strain of the DIC technique [39]. (b1) A modified SPR consisting of two washers [40]. (b2) Detailed failure morphology of the CFRP plate [40]

Fig. 7 a Schematic cross section of an SPR joint. **b** Cross section of an SPR joint [41]
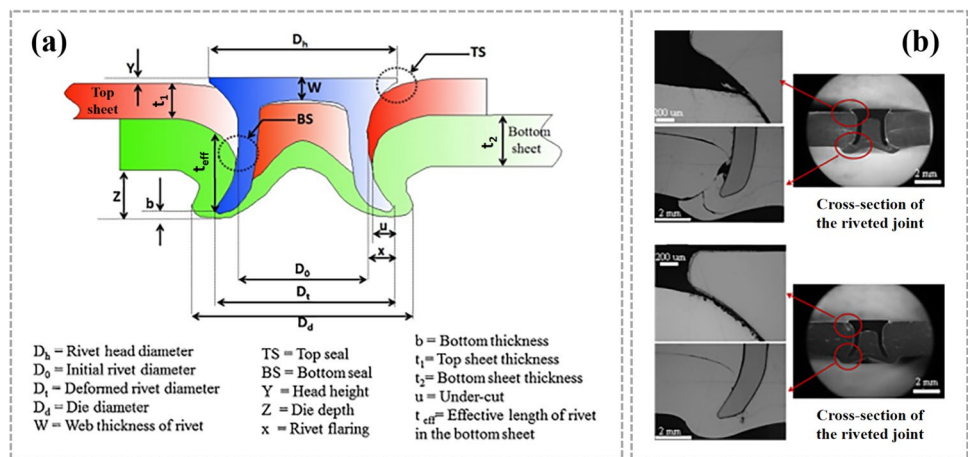
height of the DZ cavity center bulge, because the contact between the bottom sheet and the central bulge of the DZ die increased the reaction force, thus the cavity diameter and the projection height of the die were increased in the trial and error experiment. Besides, they also optimized

the die size based on the numerical method. The interlock and the forming quality of the self-piercing riveting joint have been significantly improved after optimization for the die size. The results show that the DZ die has a better joint effect in comparison to the FM die. However, it is necessary

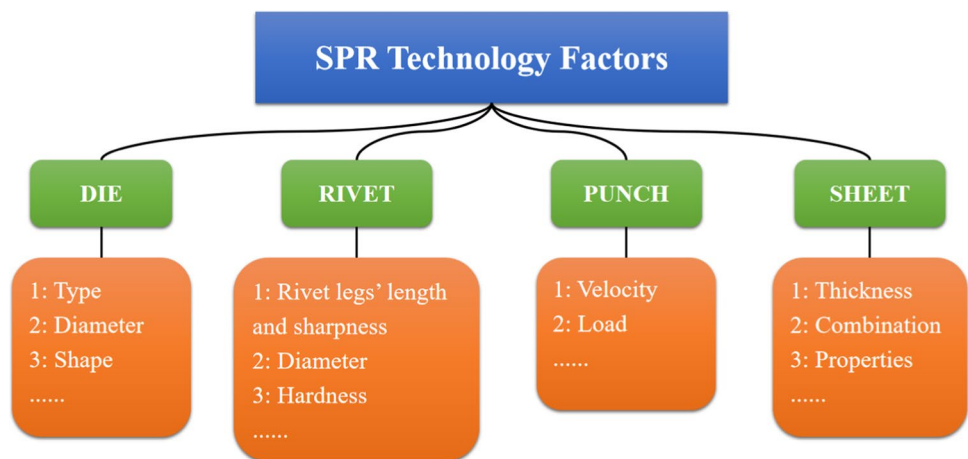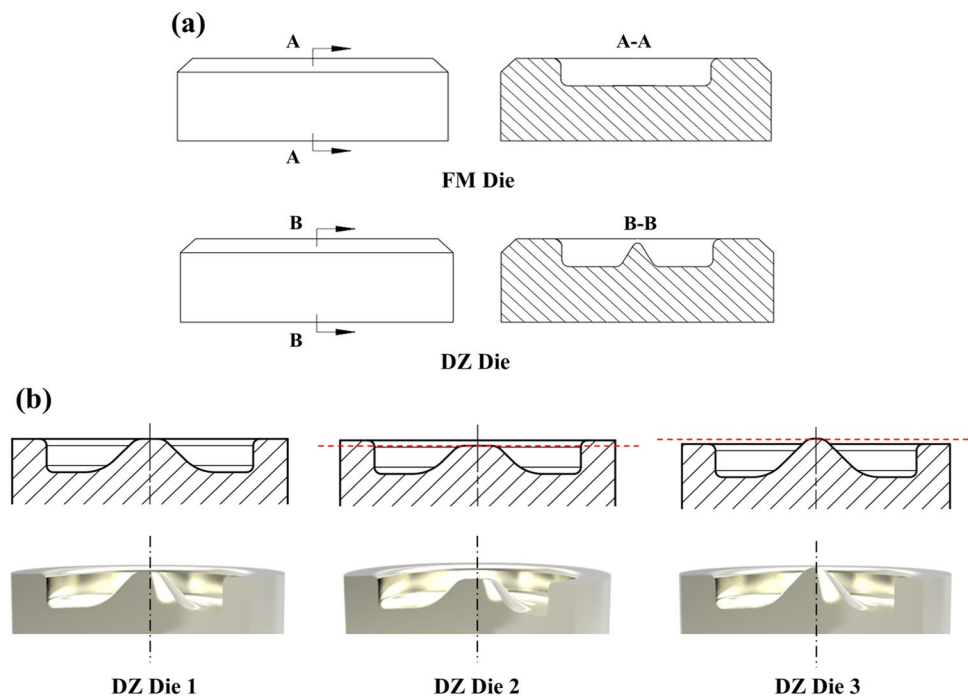**Fig. 8** Technological factors of SPR technology

Fig. 9 **a** Two types of SPR die. **b** Three profiles of SPR DZ dies

to use the FM die to produce products with higher surface smoothness requirements.

In terms of characteristics of the DZ die, Mucha [43] utilized five DZ dies with different contour parameters to investigate its influences on the quality of self-piercing riveting joints under different connection conditions. The forming quality of joints was analyzed from multiple perspectives including the riveting force and displacement, the distribution of plastic strain on the rivet, and the indentation of a joint. Ultimately, the optimal riveting joint was determined from these five different dies. Xu [44] designed three dies with different tapers to investigate the influencing factors of SPR joint quality, as shown in Fig. 9b. The bottom thickness value b is the smallest, and the

under-cut value u is the largest when using Die-1. Conversely, the bottom thickness value b is the smallest, and the under-cut value u is the largest when using Die-2. When using Die-3, the rivet flaring value x is the biggest and the Die-2 acquired the smallest rivet flaring value x. Pickin et al. [45] analyzed the effects of a series of dies with different diameters, depths, and heights on riveting joints when performing self-piercing riveting connections for sandwich panels and aluminum alloys. The results show that by changing the shape of the die, the diameter of the leg D_t can be changed after the rivet deformation. The ratio of the rivet flaring increases with the increasing internal diameter of the die.

From the above research results on different dies, it is mentioned that directly changing the size of the die can

indirectly change the deformation behavior of the rivet in the riveting process. Thus, the whole joint quality is closely related to the rivet itself. Therefore, some scholars have directly analyzed the properties of the rivet and concluded that some factors of the rivet affect the quality of SPR joint in riveting. Li et al. [46] studied the effect of the geometry of rivets on the quality of SPR joints. They introduced different specifications of rivet legs with different sharpness levels and further designed unique fixtures to ensure that the position of rivets remains fixed during the riveting process. The riveting specimens use a servo-driven riveting system produced by the Henrob company. It is concluded that sharper rivet legs undergo more significant deformation during the riveting process, i.e., the leg diameter D_t is more significant, which makes the interlock value of joint u and the remaining thickness of the bottom sheet b thicker, and significantly increases the reliability of the joint. Haque [41] analyzed the impact of the riveting quality with different hardness. The findings revealed that the use of softer rivets resulted in a slight increase in the required riveting force, which was observed through the force–displacement curve of the single-lap test. This increase was attributed to the significant deformation experienced by the softer rivets. The flaring value x of the rivet leg and the under-cut u in the bottom sheet are also increasing accordingly to improve the quality of the riveting joint. Additionally, it should be noticed that the hardness of rivet cannot be lower than the minimum requirements of the actual connection condition under the above premise.

Besides, another important factor depends on the punch speed and punching pressure. Liu et al. [47] investigated the effects of spindle rotation and rivet punch speed when studying the influencing factors of the self-piercing riveting process for heterogeneous materials. It is concluded that spindle rotation and punch speed are critical factors affecting the quality of the joint. The high spindle rotation speed and punch speed reduce axial force and torque. In contrast, low axial force correspondingly leads to a reduction in interlock. Haque et al. [48] summarized the influencing factors of self-piercing riveting joint quality in a review, of which punch pressure and punch speed are two crucial factors affecting the quality of SPR joints, and gave the following conclusions:

a. Punch pressure and punch speed can affect the quality of the SPR joint. Excessive pressure may lead to cracks in the joint, and insufficient pressure would lead to an incomplete joint connection. Therefore, before performing the self-piercing riveting connection, trial and error experiments must be carried out to obtain the optimal punch pressure to meet the connection requirements.

b. The punch speed changes the geometry of the connecting joint. For example, at high speeds (100 m/s), any

impact on the slight displacement of the upper sheet is minimized. The rivet will directly cut off the upper sheet during the initial riveting process. However, at standard speed (10–30 m/s), the rivet will have an axial stretching effect on the upper sheet. Simultaneously, the geometry of the joint will change significantly, and the deformation rate of the impact riveting will be higher. At this standard punch speed, the strength of the SPR joint will be higher since the plastic deformation of sheets is more significant to form a larger interlock structure. The remaining thickness of the bottom sheet is also larger to ensure the safety of joints.

3.2.2 Influence of the sheet material

The influence of the sheet material on the SPR joint quality mainly attributes to the inherent property of the material itself (including ductility and brittleness, etc.), the stacking order of sheets, and the thickness of the sheet. Liu et al. [47] investigated the mechanical properties and failure mechanisms of self-piercing riveting joints with CFRP and 5754 aluminum alloy. They analyzed the effect of the thickness of carbon fiber cloth and the performance of the layup angle on the joint quality. Zhang et al. [30] studied the self-piercing riveting connection technology of thermoplastic composite sheets and aluminum alloys with PA6 matrix. The glass fiber and carbon fiber composite sheet and aluminum alloy sheet are respectively connected. The stacking direction of sheets is also considered concurrently and the composite material as the upper and the bottom sheets are tested on, respectively. Through the joint cross-sectional quality and single-lap force–displacement curve analysis, the thermoplastic glass fiber reinforced composite material as the upper sheet owns a better joint forming quality when compared with the thermoplastic carbon fiber reinforced composite material. This combination makes the connection requirements easier to meet under different working conditions.

The above investigations summarize and review the joint-forming quality of SPR connection technology for heterogeneous metal composites. However, existing researches and conclusions are not limited to carbon fiber composite materials and aluminum alloys. For the joint forming quality of SPR connection for the heterogeneous sheets, the current research ideas and research priorities are in common, that is, the specific values of the joint quality are mainly evaluated and quantified through the macroscopic analysis of the surface morphology and the cross section of the joint. The specific numerical evaluation indexes are detailed in Fig. 7. Among these detailed numerical evaluation indexes, the top seal value TS, head height value Y, under-cut value u, rivet flaring value x, and bottom thickness value b are usually important indexes prioritized when evaluating the quality of joint forming.

In sum, this paper review several influencing factors of the forming quality, which are considered from the aspects of die, rivet, punch, and material, of which the die and rivet will have an impact on the quality of the joint in geometric size and shape. The punch has a specific influence on the joint quality at several aspects of the applied punch force and punch speed, as well as spindle rotation speed. As for the material factors, it is closely related to the properties of the material itself (including the ductility and brittleness of the connecting sheet), the stacking order of the sheet, and the thickness of the sheet. All the drawn conclusions apply to SPR joining technology. It should be noticed that this is still the case for self-piercing riveting of carbon fiber composites and aluminum alloys, which are summarized in Table 2.

4 Performance analysis on self-piercing riveting joints for composite and aluminum alloy

Aiming at the performance evaluation of SPR joints for carbon fiber composites and aluminum alloys, the mechanical parameters of the heterogeneous joint reach the loading requirement is a priority target. The joint is subjected to various complex loads during actual service under different working conditions. Therefore, in terms of mechanical performance analysis, the joint is mainly loaded by conventional tensile tests, including uniaxial tension and multi-angle loading by using complex fixtures. Tensile tests can provide basic information including the peak load and displacement of the joint, which can show bear capacity, the failure mode, and the damage resistance of the joint. These statistics are conducive to a complete understanding of the mechanical performance of this heterogeneous joint.

In addition to considering the external loads that the joint will be subjected to under different working conditions, the joint will face various environmental conditions throughout the entire service life. Especially for such heterogeneous materials, harsh external environments can make them highly susceptible to electrochemical corrosion. Therefore, when analyzing the performance of the heterogeneous joint, it is also important to analyze its corrosion resistance in

extreme environments. Hence, this chapter focuses on the current research progress in these two aspects separately.

4.1 Mechanical behavior and failure modes

For the performance analysis of self-piercing riveting joints, the main focus is on joint strength, plasticity, toughness, and material damage characteristics [49–52]. The main investigation methods include destructive detection and online monitoring [53]. Specifically, the destructive detection method applies destructive mechanical tests, including tensile and shear tests as well as peeling and fatigue tests, to obtain relevant joint mechanical properties and failure behavior through the cross-section. This method can also be utilized to measure crack defects and delamination modes. Indeed, the destructive detection method is the most suitable method for laboratories to study the mechanical behavior and failure modes of joints. In comparison, the online monitoring method is the most common detection method in practical applications. Its essence is to evaluate the riveting joint's behavior by detecting the stamping's force–displacement curve during the riveting process.

Di Franco et al. [54] experimentally investigated the self-piercing riveting with bonding hybrid connection for connecting carbon fiber composite sheets and aluminum alloy sheets. They first conducted a systematic test study on the lap joint to obtain the optimal way, and then they performed a tensile test on the overlapped joint. Eventually, they conducted a tensile test of the self-piercing riveting connection of carbon fiber composite material and aluminum alloy. They concluded that the damage mainly occurs in the carbon fiber composite sheet. Gay et al. [55] studied the fatigue properties of self-piercing riveting with aluminum alloy and glass fiber-reinforced thermoplastic composites. They concluded that the self-piercing riveting process can lead to damage in the composite materials, and fiber fracture and delamination are the main damage mode. Therefore, the composite material will significantly impact the limited strength of the self-piercing riveting's fatigue behavior. Aiming at the damage study of fiber-reinforced composites, relevant scholars have studied it for many years ago. Matzenmiller et al. [4] proposed a constitutive model for the anisotropic damage in fiber composites. They found a relationship between the

Table 2 Conclusion of the influencing factors on SPR of heterogeneous metal-composites sheets

|	
Die [42]	DZ-die is better than FM-die
Rivet [41, 46]	The sharper the rivet teeth make the better formability
	The lower hardness makes the better joint
Punch [48]	Proper punch-load is available through trial-and-error experiments
	Proper punch-velocity is advised at 10–30 m/s
Material [30]	High ductility is better
	The stacked sequence is top-CFRP and bottom-Al

damage and the effective elastic properties for stress analysis of the structure. The appropriate coupling between the damage variable rate equations in different damage modes is discussed. Rao et al. [56] studied the tensile and fatigue properties of continuously woven carbon fiber composite reinforcements and AA6111 single-lap joints. They found that the flatness of the rivet head has a significant linear effect on the fatigue performance of single-lap joints. The joint formed by the flat head rivet creates a larger joint on the CFRP sheet's top layer compared to the head bulge's rivet. In addition, the joint formed by the flat head rivet creates a larger joint on the top layer of the CFRP sheet than the rivet with the head bulge, resulting in lower lap shear force. Pulling out of rivets is one of the most common modes of destruction without considering the lap shear failure. At the same time, the crack propagation of the plastic deformation area of the bottom aluminum sheet is shown in Fig. 10a, which is also a cause of joint failure.

In general, fatigue failure cracks in self-piercing riveting joints occur in areas of plastic deformation close to the rivet and aluminum sheet cross section. The fracture and delamination of the fibers in the composite sheet affect the failure of the entire SPR joint. Rao et al. [57] performed quasi-static loading on the self-piercing riveting process for carbon fiber-reinforced composites when analyzing the effect of the structure of the specimen to be riveted. Two significant failure modes occurred as the rivets were pulled out of the bottom aluminum sheet resulting in a single-lap and a cross-lap joint, as is shown in Fig. 10 (b). Under cyclic load, the single-lap joint fails the kink crack propagation of the bottom aluminum sheet. In contrast, the cross-lap node fails due to the rivet pulled out of the top carbon fiber sheet.

Di Franco et al. [58] investigated the effect of rivet spacing on riveting joints when performing self-piercing riveting connections between carbon fiber composite sheets and AA2024 aluminum alloy sheets. During the entire studying of the joint failure mode, the process information was repeatedly collected by a high-definition digital camera, which aimed at monitoring the failure mode of the joint. Totally, 15 specimens were tested by using three connection methods. Particular attention is paid to the smooth treatment of the specimen sample's edges before the test to rule out the effects of small cracks that existed before the test. For more evident observation of the delamination of the composite sheet, the sides of the specimen are coated with fragile white paint, as shown in Fig. 10 (c1). Eventually, combined with the resulting joint failure diagram (as shown in Fig. 10 (c2)) and the corresponding force–displacement curve, it is

Fig. 10 (a) Propagation of the bottom aluminum sheet under the scanning electron microscope [56]. (b) Failure modes for two lapping types [57]. (c) Appearance of the sheet before and after the tensile test: (c1) test specimens, (c2) sheets after tensile failure [58]
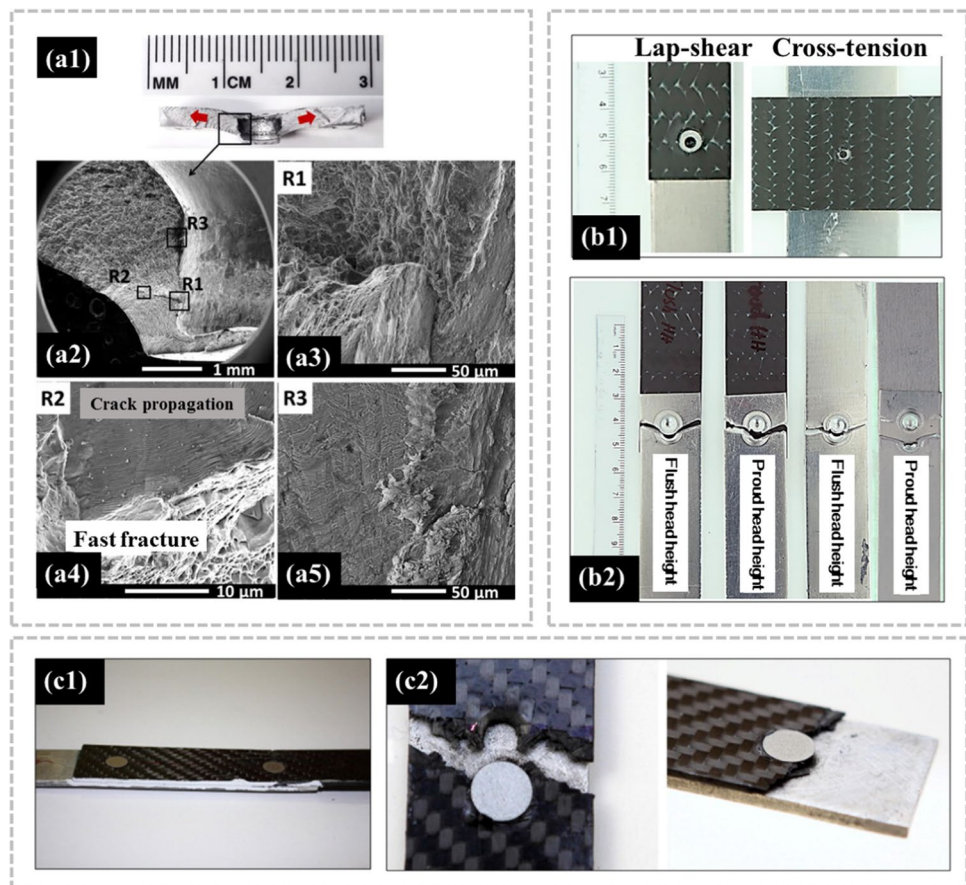
concluded that the failure of the SPR connection standard is caused by the inability between the carbon fiber sheet layers delamination near the riveting hole. On the other hand, the fracture is caused by the presence of the rivet that causes uneven stress states along the cross-section. According to the fracture theory, the geometric breaks caused by holes will result in stress concentration at their edges.

Liang et al. [59] revealed the mechanical properties and microscopic morphology of conventional riveting joints when carrying out the electromagnetic self-piercing riveting of carbon fiber composite and 5052 aluminum alloys. Based on the microscopic morphology observed as shown in Fig. 11, it is seen that CFRP breaks in the inner wall area of the rivet leg (Zone 1) and the top spot of the rivet leg (Zone 3). In addition, the damaged area is more significant. In contrast, a large bending deformation occurs in the center area of the rivet leg (Zone 2) due to more CFRP breaks in the rivet leg area in the conventional SPR joints, which is prone to the loosening and failure of joints.

In the tensile shear test conducted by the abovementioned team, it is evident that the riveting joint mainly goes through three mechanical stages in the tensile and shearing process. These stages are the elastic stage, the yield stage, and the failure stage. The elastic deformation of the stretch is mainly affected by the rivet and the bottom aluminum sheet. During the yield phase, the contact area between the aluminum sheet and the carbon fiber sheet is reduced, and the interlocking force of the joint mainly provides the shear load. Plastic deformation results in a reduced stiffness of the riveting joint. With the continuous changing of the loading rate, the shear load increases slowly in the force–displacement curve. This indicates that in the yield stage, the shear load was only related to the strength of the aluminum sheet, carbon fiber sheet, and rivet. The maximum shear force is mainly impacted in the elastic stage. As the tensile and shear test continues, the shear load begins to decrease until the interlocking structure of the joint is destroyed, and the joint fails.

In addition, Kang et al. [60] investigated the tensile and fatigue behavior of self-piercing riveting connections for automotive carbon fiber-reinforced materials and aluminum alloys. In a single-lap tensile and shear test, a force curve over time and a specimen after stretching are obtained, as shown in Fig. 12a. It is observed that the CFRP around the rivet has been damaged due to being less ductile than steel. During the stretching process, the compressive force applied by the rivet to the CFRP sheet causes the rivet head to penetrate the CFRP sheet. Ultimately, this causes delamination of the carbon fiber and further causes the rivet to be pulled out of the CFRP sheet. This mode of fiber failure is due to the squeeze of the carbon fiber sheet called bearing failure. In the fatigue performance test, it is found that the primary failure mode is that the fatigue crack spread along the width of the bottom aluminum sheet in a torsional manner. The fatigue crack occurred in a high-stress concentration area with plastic deformation near the interlocking position of the

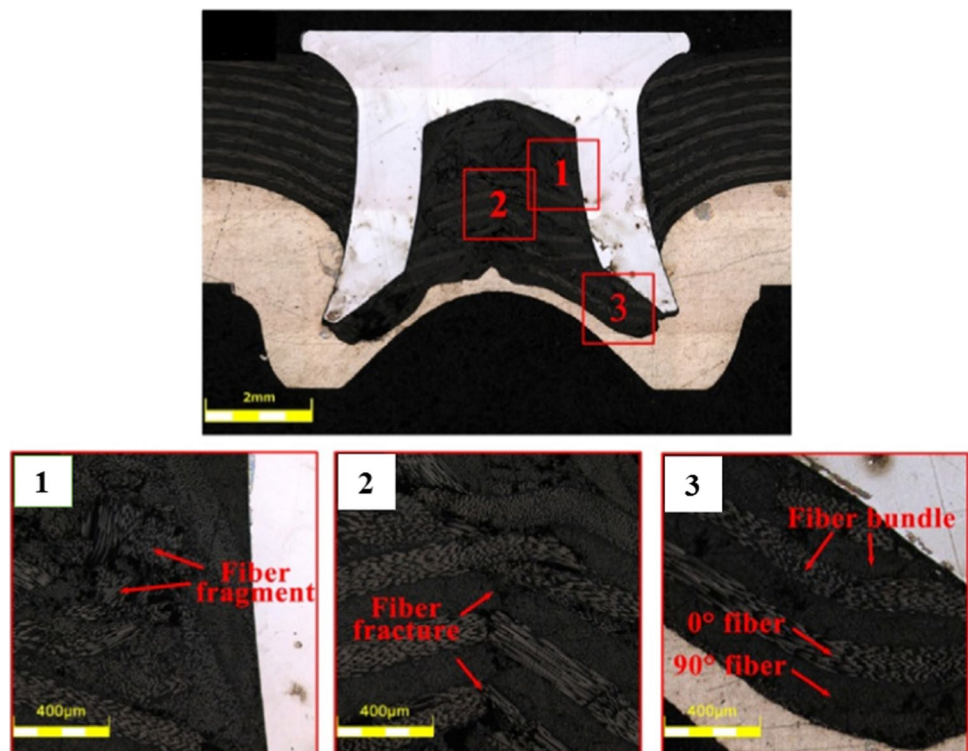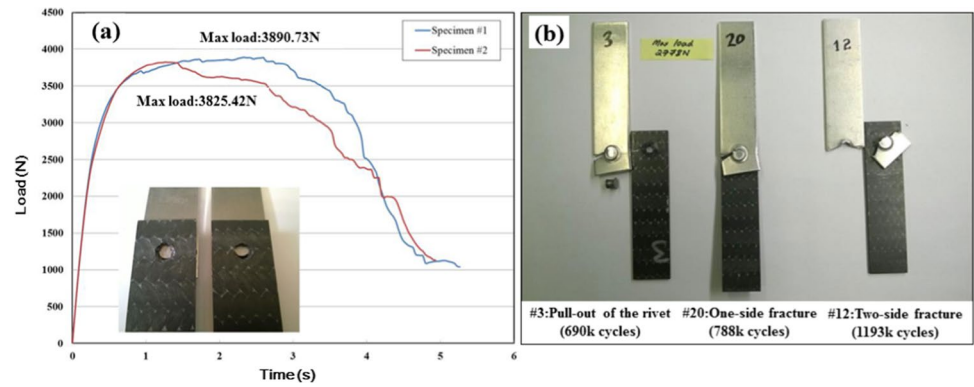**Fig. 11** Micromorphology of the riveting joint cross section and its specific area [59]

Fig. 12 **a** Failure specimen and load-time curve after single-lap tensile and shear test. **b** Fatigue specimens [60]

rivet and the bottom aluminum sheet, as shown in Fig. 12b, which is consistent with the theoretical situation.

Kroll et al. [49] explored the variation of the mechanical properties of the joint with the direction of the fiber in the study of SPR with CFRP and aluminum alloy sheets. They applied finite element simulations to assist understand the underlying mechanical properties. It is found that the mechanical behaviors of the joint reach their best when the fiber direction was chosen 0°. The area of carbon fiber lamellar structure failure in the joint was revealed in their work, which is concentrated in the inner wall of the rivet leg and the top area of the rivet leg. However, the destruction of the carbon fiber lamellar structure is less affected by the fiber direction, thus the layup orientation of the carbon fiber is not a key influencing factor on the strength of the SPR joints. In addition, other scholars' studies [29, 61, 62] also detailed the characterization of the mechanical properties and the failure modes of self-piercing riveting joints with composites and metals. Experimental tests, numerical simulations, and sampled the cross section of joints by scanning electron microscope were severally conducted. It is concluded that the interlayer fracture and delamination of carbon fiber-reinforced plastic occur when the SPR joint is destroyed. The rivets have two failure situations: pull-out and bearing failure due to the destruction of carbon fiber sheets.

It can be accomplished through the common single-lap joint to analyze the bearing failure mode of the SPR joints. However, this simple overlap method is difficult to meet the needs for the pull-out failure mode analysis. In response to this situation, many scholars have improved the experimental fixture proposed by Arcan [65], which can achieve complex loading conditions such as tension and shear. Xue et al. [63] used the improved Arcan fixture in the study of steel-aluminum self-piercing riveted joints, as shown in Fig. 13a, where the 0° direction can be used for pull-out failure mode. Similarly, Leconte et al. [64] designed a similar Arcan fixture to test the mechanical performance of joint pure shear, pure tension, and mixed tension-shear loading conditions in the study of self-piercing riveting for aluminum alloy and PA66, as shown in Fig. 13b. After conducting tensile-shear tests on carbon fiber and aluminum alloy plates joined by the above-mentioned experimental fixtures, the results showed that the maximum load-bearing capacity of the joint was about 4500N. Indeed, the specific value will be relevant to the different thicknesses of the riveting sheet and the size of the rivet.

To sum up, from the perspective of the force–displacement curve of a tensile test, the whole tensile process can be divided into the elastic stage, yield stage, and failure stage. When the early tensile load is small, the elastic deformation of the joint is mainly affected by the rivet and the bottom aluminum sheet due to the rivet and the aluminum sheet are metal materials with prominent elastoplastic properties. However, as the tensile load increases, it enters the yield stage, where the corresponding contact area between the aluminum sheet and the carbon fiber sheet is reduced. The

Fig. 13 Improved Arcan fixture for SPR mode test of the SPR joint [63, 64]
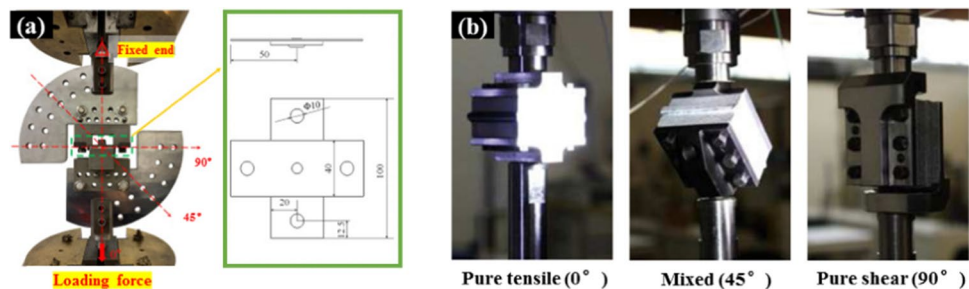
interlocking force of the joint mainly provides the shear load and plastic deformation results in a reduced stiffness of the riveting joint. As the tensile load increases, the shear load increases slowly in the force–displacement curve. This shows that in the yield stage, the shear force is only related to the strength of the aluminum sheet, carbon fiber sheet, and rivet, and has a decisive impact on the maximum shear force of the joint in the elastic stage. When the load continues to increase, the compression force of the rivet to the carbon fiber sheet leads to interlayer fracture and delamination and two typical failure modes of rivet would occur due to the stiffness of the rivet being greater than that of the carbon fiber sheet. Therefore, the damage to the carbon fiber sheet is a decisive factor affecting the mechanical performance of the joint. Besides, the carbon fiber sheet will also cause the fiber layer to be bent and break in the inner wall of the rivet leg and the top of the leg due to the normal force of the rivet. It is unavoidable because the carbon fiber sheet, as the upper sheet of the riveting, must go through the process of being penetrated by the rivet, so the interlayer fracture is inevitable, thus the fiber fracture area is concentrated inside the semi-hollow rivet. In contrast, the rivet leg forms an interlocking structure in the bottom aluminum sheet, directly inhibiting the expansion of fiber fracture and layering. Therefore, this phenomenon does not degrade the performance of the SPR joint.

4.2 Corrosion resistance of self-piercing riveting joints

The abovementioned discussions have analyzed the mechanical behavior and the failure mode of the self-piercing riveting joint of carbon fiber-reinforced plastic and aluminum alloy under tensile conditions in good laboratory environments. However, the practical working environment of the self-piercing riveting joint should be more rigorous, such as the possibilities of facing thermal temperature, high pressure, and especially corrosions, etc. Hence, the corrosion resistance investigation of the SPR joint is essential. It is necessary to explore the mechanics and service performance of corroded self-piercing riveting joints in severe corrosive environments and also to analyze the corrosion failure mechanism based on microstructure observations[66–68].

Nowadays, Mandel et al. [69, 70] numerically simulated the galvanic corrosion process of self-piercing riveting for 6060 aluminum alloys and carbon fiber-reinforced plastics. The potentiodynamic polarization method determined the corrosion parameters of the joint components required for finite element simulation. Immersion tests in the constant environment ultimately determined the critical distance for electronic pitting on the aluminum alloy surface. They conducted a long-term corrosive study on the self-piercing riveting connections of two types of material, as shown in Fig. 14 (a1). Specifically, they used VDA 621–415 climate chamber multi-corrosion cycle test to study the corrosion behavior of 6060-T6 aluminum alloy in self-piercing riveting connections. After each cycle, the most damaged area of the aluminum alloy was found close to the overlapping part. The damage evolution was assessed by interferometry, and the volume at the pitting corrosion was subsequently calculated. In addition, the potential dynamic polarization behavior of each joint component was analyzed in the salt spray test using 5 wt.% sodium chloride solution according to the guidance of VDA 621–415, as shown in Fig. 14 (a2). Through the graphical exploration of the polarization curve, the galvanic corrosion characteristics are detected, and the pitting sensitivity of aluminum alloy in the joint is evaluated.

Abdul Karim et al. [71] assessed the effect of corrosion of different riveting layers on the strength degradation of CFRP/Al self-piercing riveting joints. Two other layers of Almac® and Zn-Ni rivets for self-piercing riveting connections were utilized. After 13 weeks of accelerated corrosion testing, they summarized the joints' corrosion and strength degradation characteristics, as shown in Fig. 14 (b). The experimental results show that the strength loss of Almac-coated® SPR joints is at least three times that of the Zn-Ni-coated SPR joints. Corrosion product characterization and potentiodynamic polarization tests reveal corrosion mechanisms. A solid galvanic coupling between the Almac-coated® rivet head and the CFRP sheet accelerates the dissolution of the rivet head coating. It triggers corrosion of the rivet substrate (steel) early in the test. As a result, the interlock between the rivet legs and the bottom sheet is significantly weakened, and the loss of strength is significant. In contrast, the riveting of the Zn-Ni coating improves the corrosion resistance of the SPR connection due to the weak electrical coupling between the coated surface and the rivet.

In summary, since the practical industrial environment is much harsher than the laboratory environment, it is necessary to conduct the corrosion resistance evaluation on SPR joints, to understand the corrosion conditions of the joints in various environmental conditions and then pretreat the joints accordingly to prevent corrosion. However, because the external environment is uncontrollable, the riveting material has been determined to improve the corrosion resistance of the self-piercing riveting joint; the rivet is currently used for plating treatment. Moreover, different coatings have different corrosion resistance, and the specific type of anti-corrosion coating used for the corresponding working conditions needs to be determined by experiments according to the specific working environment.

Fig. 14 Photograph of the transition from the overlap to the zone of field-dependent pitting sensitivity [69]. (a1) SEM image of pitting corrosion at the aluminum alloy. (a2) After 6 weeks immersion in 5 wt.% NaCl solution. (b) Cross-sectional images of the rivet head for the initial state and after 13 weeks of the salt spray test [71]: (b1) Almac® SPR joints, (b2) Zn-Ni-coated SPR joints
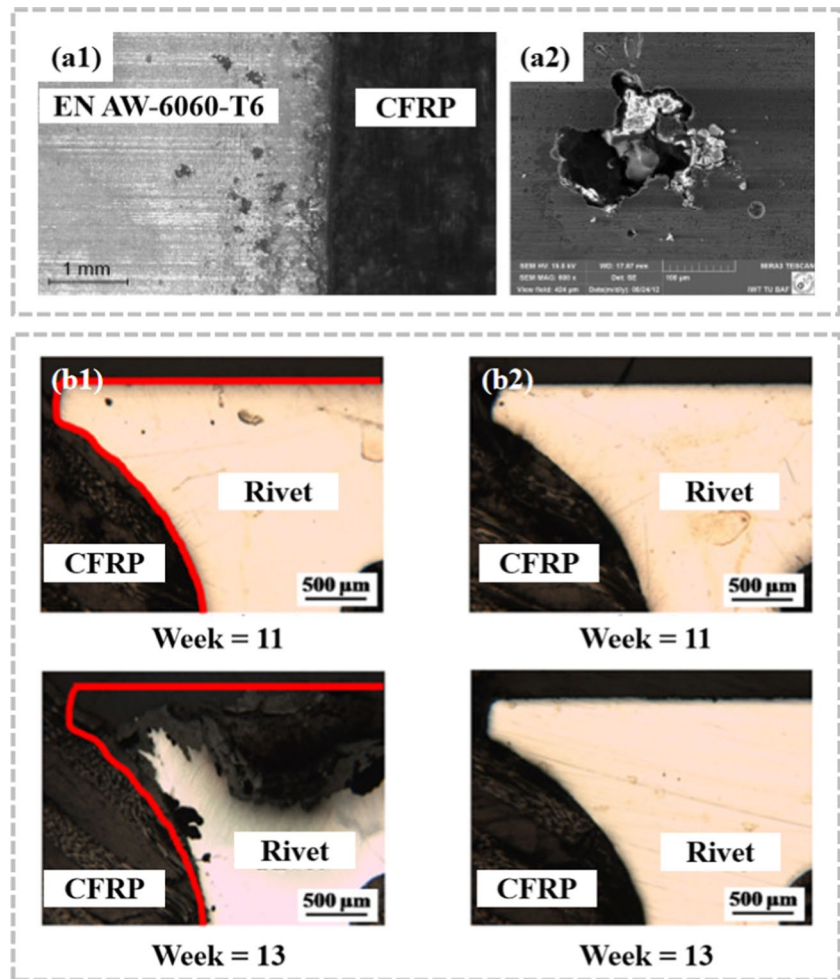
5 Numerical investigation of self-piercing riveting for carbon fiber reinforced plastic and aluminum

The numerical approach is vital for the development of new products. Its application scope is broad, which includes various scientific and technological fields such as automotive, aerospace, biomedicine, electrical and electronics, etc. Appropriate commercial software should be selected to complete the simulation analysis tasks based on practical needs. Currently, computer-aided design combined with computer-aided engineering (especially finite element methods) is highly competitive to develop new products rapidly and reduce costs. At present, the numerical simulation based on commonly used commercial finite element analysis software typically goes through three stages: pre-processing, solution process, and visual post-processing. The most important stage is the pre-processing stage, which directly determines the reliability of the numerical results. Besides, appropriate simplification of the pre-processing stage can greatly improve the calculation efficiency. The current commercial software such as Ls-Dyna, Ansys, and ABAQUS, etc. are usually used for numerical simulation of self-piercing riveting connections because of their robustness and huge material libraries options, which are summarized in Table 3. Furthermore, users can develop their subroutines for specific material constitutive models as well.

A brief analysis of the numerical simulation for the self-piercing riveting process is presented: In the modeling strategy, two-dimensional modeling is usually simplified by axis symmetry. In contrast, 3D modeling can be calculated by taking a quarter of the entire model, which can significantly improve the calculation efficiency. Specifically, the effective active area of the self-piercing riveting process can be regarded as a rotary body. Furthermore, the complete visualization of results can be obtained by reflecting the symmetrical surface post-processing, which is also recommended. Secondly, suppose the sheet's material is isotropic. In that case, it can be modeled by a two-dimensional axisymmetric method. If the sheet's material is anisotropic, it is necessary to consider three-dimensional modeling, as shown in Table 4.

The difficulty in numerical modeling the SPR connection between fiber-reinforced composite materials and metals is

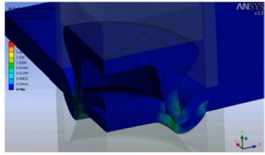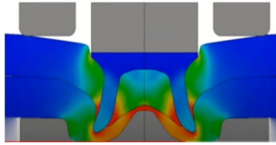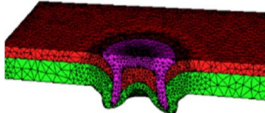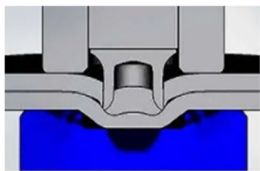**Table 3** Summary of commercial software for SPR simulation
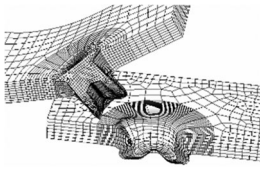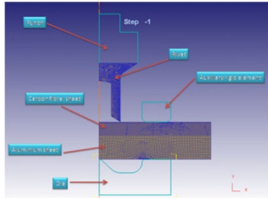
Software Type	Legend
ANSYS [72]	
LS-DYNA [73]	
Forge2005® [74]	
Simufact [75]	
ABAQUS [76]	
DEFORM 2D [29]	

Table 4 Recommendations of SPR simulation

Sheet property	2D model	3D model	Whether simplified
Isotropic material	√	√	√
Anisotropic material	×	√	√

mainly ascribed to the difference in the material properties and contact conditions of multifarious materials definitions. Besides, for the anisotropic characteristics and mechanisms of fiber-reinforced composites, it must be considered the more complex forming and failure behaviors in numerical simulations, in contrast to SPR connection for homogeneous metals where the material can be simplistically set as isotropic.

Relevant numerical research for modeling the SPR connection is briefly summarized as follows. For instance, Bouchard et al. [74] performed a numerical analysis from riveting process modeling to structural analysis, focusing on numerical simulation of the SPR process and analyzing the mechanical strength after the final riveting. They considered the contact conditions, material plastic deformation, damage, and fracture between the deformed bodies within their numerical simulations. Hence, they initially simulated a 2D riveting process and then introduced the stress field into a three-dimensional mesh analysis. After that, they performed a three-dimensional shear test on the riveted structure. In this way, the transport of the stress field, such as residual stress or damage, can be examined for the effect of the final mechanical strength of the riveting specimen, and the structural stability of the SPR connection can be successfully predicted. Even more, Casalino et al. [77] further provided a scientific description for modeling the simulation of a self-piercing riveting process. The simulation process was carried out by using LS-DYNA software, and the accuracy of the results was validated by comparing them to experimental data.

For the numerical simulations of the SPR process involving the composite materials, it is necessary to consider the failure analysis of composite materials. It is worth mentioning that the failure analysis of FRP requires the consideration of nonlinear stress and strain relationship. In determining laminate design and FRP safety factors, accurate fracture criteria and degradation models are urgently needed to simulate the brittle failure behavior of composites. As early as in the last century, scholars have proposed a series of failure criteria between fibers [78], which provide the realistic stress for destruction and indicate the direction of cracks. Within the fiber layer and after cracking occurs, the laminate gradually degrades with the increasing load until the fiber breaks on a specific layer, which causes the final delamination of the fiber layers. To accurately characterize the failure and damage behavior of carbon fiber composites at the joining position based on self-piercing riveting, three-dimensional modeling is necessary to contain the anisotropic material properties of composite materials, such as in the work of Drossel et al.[79], where the numerical simulation models of the self-piercing riveting joining process of carbon fiber-reinforced plastics and aluminum alloys are developed. Since the entire model is a rotary body and requires a large number of meshes and contacts to be analyzed when conducting 3D simulation. To simplify, it is necessary to perform a quarter modeling strategy, as shown in Fig. 15 (a1–a3). They completed the solution calculations with the LS-DYNA solver and simulated results show that is highly consistent with the experimental results. The results addressed that the accumulation of fiber breaks concentrates upon the semi-hollow region of the rivet, and the rivet leg
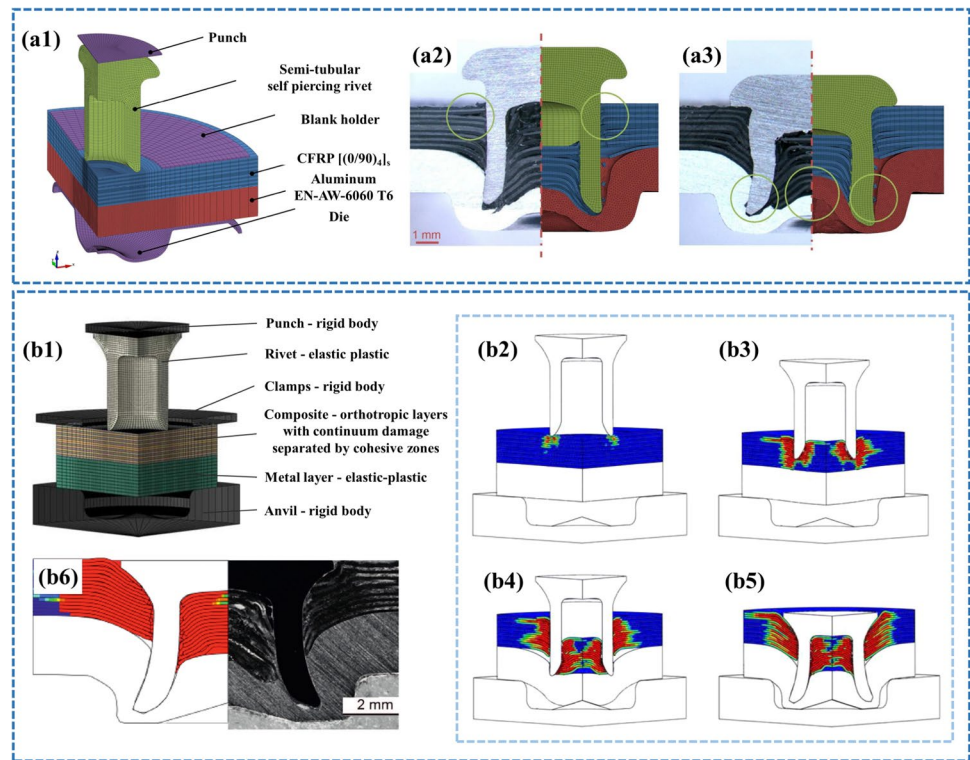
flaring is detailed simulated which is following the actual experimental situation.

Hirsch et al. [31] also focused on the deformation and destruction behavior of composites during numerical simulations of self-piercing riveting connections between fiber-reinforced plastics and metal sheets. Unlike the simulation for metal self-piercing riveting processes, which only focus on large plastic deformations, the mechanical response of composites is often determined by the damage within layers. Depending on the polymer matrix, viscoelastic effects can exceptionally affect the long-term performance of the joint. Therefore, scholars introduced subroutines and homogenization techniques to predict the mechanical properties of composite materials according to the properties of effective anisotropic elastic or viscoelastic materials. Through coupling it with the continuous damage method (CDM), an accurate model representing the deformation and destruction of a single sheet layer was established to effectively simulate the interfacial adhesive delamination behavior of the cohesive region. The corresponding simulation results are shown in Fig. 15 (b). Similarly, Rao et al. [80] numerically investigated the SPR connection for carbon fiber-reinforced plastics to understand the strengthening mechanism of joints. They adjusted the geometry of the rivet to complete the corresponding simulation analysis based on LS-DYNA software.

From the above research, it can be seen that the development of numerical approaches especially through numerical simulation to assist the investigation of SPR connections for heterogeneous CFRP/metal materials has already opened a convenient door for the riveting modeling field. Especially, current numerical analysis methods are highly mature and can utilize existing constitutive models such as the Johnson–Cook model, Zerilli-Armstrong model, Maewaka model, and Nemat-Nasser model to accurately predict the corresponding elastic–plastic mechanical behavior of metallic materials. Simultaneously, several criteria are also available for modeling composite materials, including the Tsai-Hill criterion, Puck failure criterion, Pinho theory, and Hashin criterion. Nevertheless, numerical analysis of composite materials is relatively complex due to it requires consideration of the coupled interaction of fiber and matrix failure. Mostly commercial finite element software only integrates simplified 2D criteria, such as Pinho theory's 2D criterion in ABAQUS and Ls-Dyna, and Hashin failure criterion's 2D criterion in ABAQUS and MSC.Dytran. More accurate 3D criteria for failure prediction of composites mostly require users to program subroutines, which demands scholars to have abundant theoretical and mechanical knowledge.

Despite the extensive research on failure theories of different composite materials, this field is still in a stage of vigorous development, and no universal theory can be applied to model different riveting conditions. Therefore, when conducting a simulated procedure of CFRP/metal SPR connections, the difficulty and focus lie in setting the properties of composite materials and requiring a large number of

experiments to obtain valid data. It is also necessary to select appropriate material constitutive models and failure criteria specifically. Especially, no suitable constitutive model is integrated into existing commercial software to describe thermoplastic carbon fiber composite materials. Therefore, researchers need to develop indispensable subroutines independently. In sum, there is still ample room for development in the field of numerical modeling for the SPR connection composite materials and metals, particularly in developing composite material failure models, which is highly valuable for in-depth and accurate research.

6 Conclusions

With the wide application prospects of self-piercing riveting connection technology for heterogeneous materials in automobiles, aircraft, and other fields, this paper provides a detailed review of SPR for composite materials and aluminum alloy sheets for the relevant research done by scholars in the recent decade. Specifically, it summarizes some existing research and provides perspectives for corresponding research in this field. The conclusions of this paper are summarized as follows:

> The process of the self-piercing riveting technology and the related widely used equipment specifications are summarized in detail. Self-piercing riveting process is divided into four steps: sheet positioning and rivet-edge pressing, pressure maintenance, unloading, and punch releasing. The riveting equipment is the main root of Henrob company, which mainly produces semi-hollow rivets and the corresponding riveting machine. A good deal of research introduces Henrob's products as a reference standard.
>
> Since the self-piercing riveting for CFRP and aluminum alloys connection is an innovative joining process, the feasibility of this process can be characterized by the forming quality of the joint. Specifically for riveting the CFRP sheet and aluminum alloy sheet together, the carbon fiber sheet must be placed on the top due to the poor formability of the carbon fiber composites. Otherwise, the carbon fiber sheet can be easily pierced and cracked due to the complex deformation of the rivet legs during the SPR process. The evaluation method of the SPR joint quality aiming at the CFRP-metal joint is entirely consistent with which of the metal-to-metal SPR joint, mainly by measuring the head height after riveting, the flaring degree, and the interlock value of the rivet legs. In addition, the residual thickness of the bottom aluminum sheet is also critical to quantify the joint forming quality. The crucial factors directly impacting

the above-mentioned geometrical parameters include the shape of the die, the size of the rivet, the punch force as well as the material type of sheet.

> For ensuring a valid self-piercing riveting connection, the joint performance needs to be investigated to effectively evaluate the reliability of the SPR joint. Limited by the low plasticity of carbon fiber sheets, single-lap tensile and shear experiments are usually utilized to evaluate the mechanical properties and corresponding failure modes of joints. In the tensile process, the joint undergoes three stages including elastic deformation, yielding, and finally failure. Based on the phenomena of interlayer fracture and delamination within the carbon fiber sheets, joint failure is divided into two modes: bearing failure and pull-out failure. It is mentioned that to ensure the effectiveness and reliability of the SPR connection. Besides, it is necessary to carry out corrosion resistance studies for the SPR connection in extreme environments. The corrosion resistance can be improved by adding a coating layer on the rivet.
>
> Since the anisotropic material properties of composites are needed to be considered during numerical simulation, it is necessary to carry out three-dimensional modeling for the parts of the SPR riveting including rivet, die, sheets, etc. Moreover, it is necessary to divide the entire three-dimensional model into quarters to improve the simulation efficiency.

References

1. Tisza M, Czinege I (2018) Comparative study of the application of steels and aluminium in lightweight production of automotive parts. Int J Light Mater Manuf 1:229–238. https://doi.org/10.1016/j.ijlmm.2018.09.001

2. Miller WS, Zhuang L, Bottema J, Wittebrood AJ, Smet P, Haszler A, Vieregge A (2000) Recent development in aluminium alloys for the automotive industry. Mater Sci Eng A Struct Mater 280:37–49. https://doi.org/10.1016/S0921-5093(99)00653-X

3. Sim K-B, Baek D, Shin J-H, Shim G-S, Jang S-W, Kim H-J, Hwang J-W, Roh J-U (2020) Enhanced surface properties of carbon fiber reinforced plastic by epoxy modified primer with plasma for automotive applications. Polymers (Basel) 12:556. https://doi.org/10.3390/polym12030556

4. Matzenmiller A, Lubliner J, Taylor RL (1995) A constitutive model for anisotropic damage in fiber-composites. Mech Mater 20:125–152. https://doi.org/10.1016/0167-6636(94)00053-0

5. Shamloo A, Fathi B, Elkoun S, Rodrigue D, Soldera A (2018) Impact of compression molding conditions on the thermal and mechanical properties of polyethylene. J Appl Polym Sci 135:46176. https://doi.org/10.1002/app.46176

6. Vorderbrüggen J, Meschut G (2019) Investigations on a material-specific joining technology for CFRP hybrid joints along the automotive process chain. Compos Struct 230:111533. https://doi.org/10.1016/j.compstruct.2019.111533

7. Zhang DW, Zhang Q, Fan X, Zhao S (2019) Review on joining process of carbon fiber-reinforced polymer and metal: applications and outlook. Rare Metal Mat Eng 48:44–54

8. Cui J, Gao S, Jiang H, Huang X, Lu G, Li G (2020) Adhesive bond-electromagnetic rivet hybrid joining technique for CFRP/Al structure: process, design and property. Compos Struct 244:112316. https://doi.org/10.1016/j.compstruct.2020.112316

9. Elmarakbi A (2012) Crashworthness analysis of composite and thermoplastic foam structure for automotive bumper subsystem. Adv Compos Mater Automot Appl. https://doi.org/10.1002/9781118535288.ch6

10. Kim HC, Shin DK, Lee JJ, Kwon JB (2014) Crashworthiness of aluminum/CFRP square hollow section beam under axial impact loading for crash box application. Compos Struct 112:1–10. https://doi.org/10.1016/j.compstruct.2014.01.042

11. Gao Y, Liu Z, Xu Y, Xu X, Feng Z (2020) Research on the application of CFRP in automobile panels. Automot Eng 42:978–984. https://doi.org/10.19562/j.chinasae.qcgc.2020.07.019

12. Zang J, Zhou J, Qiu R (2020) Integrated optimization design of structure/material of CFRP automobile collision avoidance beam. Mach Des & Manuf 8:206–210. https://doi.org/10.19356/j.cnki.1001-3997.2020.08.048

13. Sun G, Li S, Liu Q et al (2016) Experimental study on crashworthiness of empty/aluminum foam/honeycomb-filled CFRP tubes. Compos Struct 152:969–993. https://doi.org/10.1016/j.compstruct.2016.06.019

14. Qin G, Na J, Mu W, Tan W (2019) Effect of thermal cycling on the degradation of adhesively bonded CFRP/aluminum alloy joints for automobiles. Int J Adhes Adhes 95:102439. https://doi.org/10.1016/j.ijadhadh.2019.102439

15. Mori K, Bay N, Fratini L, Micari F, Tekkaya AE (2013) Joining by plastic deformation. CIRP Ann 62:673–694. https://doi.org/10.1016/j.cirp.2013.05.004

16. Zheng G, He Z, Wang K, Liu X, Luo Q, Li Q, Sun G (2021) On failure mechanisms in CFRP/Al adhesive joints after hygrothermal aging degradation following by mechanical tests. Thin-Walled Struct 158:107184. https://doi.org/10.1016/j.tws.2020.107184

17. Ren S, Ma Y, Saeki S, Iwamoto Y, Chen C, Ma N (2020) Fracture mechanism and strength evaluation of Al5052/CFRP joint produced by coaxial one-side resistance spot welding. Compos Struct 252:112766. https://doi.org/10.1016/j.compstruct.2020.112766

18. Kumar S, Avinash G, Vimal E (2020) Ductility effect on clinching joint strength in lap-shear configuration loading. Mater Today Proc. https://doi.org/10.1016/j.matpr.2020.06.144

19. Lambiase F, Di Ilio A (2016) Damage analysis in mechanical clinching: experimental and numerical study. J Mater Process Technol 230:109–120. https://doi.org/10.1016/j.jmatprotec.2015.11.013

20. Jäckel M, Maul S, Kraus C, Drossel W-G (2018) Numerical simulation of thermal supported self-pierce riveting of an ultra high-strength aluminium alloy. J Phys Conf Ser 1063:12074. https://doi.org/10.1088/1742-6596/1063/1/012074

21. Durandet Y, Deam R, Beer A, Song W, Blacket S (2010) Laser assisted self-pierce riveting of AZ31 magnesium alloy strips. Mater Des 31:S13–S16. https://doi.org/10.1016/j.matdes.2009.10.038

22. Zhuang W (2018) Joint performance analysis on connection of ultrahigh-strength steel and aluminum alloy with hot riveting. J JiLin Univ 4:8

23. Ying L, Gao T, Dai M, Hu P, Dai J (2021) Towards joinability of thermal self-piercing riveting for AA7075-T6 aluminum alloy sheets under quasi-static loading conditions. Int J Mech Sci 189:105978. https://doi.org/10.1016/j.ijmecsci.2020.105978

24. Fuhrmeister R (1977) Method and apparatus for riveting, US Patent: US19770788645A

25. Porcaro R, Hanssen AG, Langseth M, Aalberg A (2006) Self-piercing riveting process: an experimental and numerical investigation. J Mater Process Technol 171:10–20. https://doi.org/10.1016/j.jmatprotec.2005.05.048

26. Hoang NH, Porcaro R, Langseth M, Hanssen AG (2010) Self-piercing riveting connections using aluminium rivets. Int J Solids Struct 47:427–439. https://doi.org/10.1016/j.ijsolstr.2009.10.009

27. Mori K, Abe Y, Kato T (2014) Self-pierce riveting of multiple steel and aluminium alloy sheets. J Mater Process Technol 214:2002–2008. https://doi.org/10.1016/j.jmatprotec.2013.09.007

28. He X, Zhao L, Deng C, Xing B, Gu F, Ball A (2015) Self-piercing riveting of similar and dissimilar metal sheets of aluminum alloy and copper alloy. Mater Des 65:923–933. https://doi.org/10.1016/j.matdes.2014.10.002

29. Di Franco G, Fratini L, Pasta A, Ruisi VF (2013) On the self-piercing riveting of aluminium blanks and carbon fibre composite panels. Int J Mater Form 6:137–144. https://doi.org/10.1007/s12289-011-1067-2

30. Zhang J, Yang S (2014) Self-piercing riveting of aluminum alloy and thermoplastic composites. J Compos Mater 49:1493–1502. https://doi.org/10.1177/0021998314535456

31. Hirsch F, Müller S, Machens M, Staschko R, Fuchs N, Kästner M (2017) Simulation of self-piercing rivetting processes in fibre reinforced polymers: material modelling and parameter identification. J Mater Process Technol 241:164–177. https://doi.org/10.1016/j.jmatprotec.2016.10.010

32. Zhang X, He X, Xing B, Wei W, Lu J (2020) Pre-holed self-piercing riveting of carbon fibre reinforced polymer laminates and commercially pure titanium sheets. J Mater Process Technol 279:116550. https://doi.org/10.1016/j.jmatprotec.2019.116550

33. Li D, Chrysanthou A, Patel I, Williams G (2017) Self-piercing riveting-a review. Int J Adv Manuf Technol 92:1777–1824. https://doi.org/10.1007/s00170-017-0156-x

34. Available at: https://www.atlascopco.com/en-pk/itba/products/joining-solutions/self-pierce-riveting

35. Oh S, Kim HK, Jeong T-E, Kam D-H, Ki H (2020) Deep-learning-based predictive architectures for self-piercing riveting process. IEEE Access 8:116254–116267. https://doi.org/10.1109/ACCESS.2020.3004337

36. Zhao H, Han L, Liu Y, Liu X (2021) Quality prediction and rivet/die selection for SPR joints with artificial neural network and genetic algorithm. J Manuf Process 66:574–594. https://doi.org/10.1016/j.jmapro.2021.04.033

37. Daniel Freiberg AIGH (2021) The effect of quench parameters on self-piercing rivet joint performance in a high strength automotive 6111 aluminum alloy. SAE Int 3:1790–1800. https://doi.org/10.4271/2021-01-0273

38. Chanyang Kim KMMH (2021) Development of analytical strength estimator for self-piercing rivet joints through observation of finite element simulations. Int J Mech Sci. https://doi.org/10.1016/j.ijmecsci.2021.106499

39. Sadowski T, Knec M (2013) Application of DIC technique for monitoring of deformation process of SPR hybrid joints / Zastosowanie Techniki Dic Do Obserwacji Procesu Deformacji

Hybrydowych Połaczen Typu Spr. Arch Metall Mater 58:119–125. https://doi.org/10.2478/v10172-012-0161-x

40. Ueda M, Miyake S, Hasegawa H, Hirano Y (2012) Instantaneous mechanical fastening of quasi-isotropic CFRP laminates by a self-piercing rivet. Compos Struct 94:3388–3393. https://doi.org/10.1016/j.compstruct.2012.04.027

41. Haque R (2018) Quality of self-piercing riveting (SPR) joints from cross-sectional perspective: a review. Arch Civ Mech Eng 18:83–93. https://doi.org/10.1016/j.acme.2017.06.003

42. Mori K, Kato T, Abe Y, Ravshanbek Y (2006) Plastic joining of ultra high strength steel and aluminium alloy sheets by self piercing rivet. CIRP Annals 55:283–286. https://doi.org/10.1016/S0007-8506(07)60417-X

43. Mucha J (2011) A study of quality parameters and behaviour of self-piercing riveted aluminium sheets with different joining conditions. Strojniški Vestn - J Mech Eng 57:323–333. https://doi.org/10.5545/sv-jme.2009.043

44. Xu Y (2013) Effects of factors on physical attributes of self-piercing riveted joints. Sci Technol Weld Join 11:666–671. https://doi.org/10.1179/174329306X131866

45. Pickin CG, Young K, Tuersley I (2007) Joining of lightweight sandwich sheets to aluminium using self-pierce riveting. Mater Des 28:2361–2365. https://doi.org/10.1016/j.matdes.2006.08.003

46. Li DZ, Han L, Shergold M, Thornton M, Williams G (2013) Influence of rivet tip geometry on the joint quality and mechanical strengths of self-piercing riveted aluminium joints. Mater Sci Forum 765:746–750. https://doi.org/10.4028/www.scientific.net/MSF.765.746

47. Liu Y, Zhuang W (2019) Self-piercing riveted-bonded hybrid joining of carbon fibre reinforced polymers and aluminium alloy sheets. Thin-Walled Struct 144:106340. https://doi.org/10.1016/j.tws.2019.106340

48. Haque R, Durandet Y (2016) Strength prediction of self-pierce riveted joint in cross-tension and lap-shear. Mater Des 108:666–678. https://doi.org/10.1016/j.matdes.2016.07.029

49. Kroll L, Mueller S, Mauermann R, Gruetzner R (2011) Strength of self-piercing riveted joints for cfrp/aluminium sheets. Proceedings of 18th International Conference on Composite Materials, Jeju Island, South Korea, pp 1–6

50. Jiang H, Sun L, Liang J, Li G, Cui J (2019) Shear failure behavior of CFRP/Al and steel/Al electromagnetic self-piercing riveted joints subject to high-speed loading. Compos Struct 230:111500. https://doi.org/10.1016/j.compstruct.2019.111500

51. Wilhelm MF, Fuessel U, Richter T, Riemer M, Foerster M (2015) Analysis of the shear-out failure mode for CFRP connections joined by forming. J Compos Mater 49:981–993. https://doi.org/10.1177/0021998314528264

52. Tamboli S, Pandey A, Bongale A, Kumar S (2019) Performance evaluation of cracked aluminum alloy repaired with carbon fiber reinforced polymer for aerospace application. Mater Res Express 6:115326. https://doi.org/10.1088/2053-1591/ab493c

53. Available at: www.auto-testing.net

54. Di Franco G, Fratini L, Pasta A (2013) Analysis of the mechanical performance of hybrid (SPR/bonded) single-lap joints between CFRP panels and aluminum blanks. Int J Adhes Adhes 41:24–32. https://doi.org/10.1016/j.ijadhadh.2012.10.008

55. Gay A, Lefebvre F, Bergamo S, Valiorgue F, Chalandon P, Michel P, Bertrand P (2016) Fatigue performance of a self-piercing rivet joint between aluminum and glass fiber reinforced thermoplastic composite. Int J Fatigue 83:127–134. https://doi.org/10.1016/j.ijfatigue.2015.10.004

56. Rao HM, Kang J, Huff G, Avery K, Su X (2017) Impact of rivet head height on the tensile and fatigue properties of lap shear self-pierced riveted CFRP to aluminum. SAE Int J Mater Manuf 10:167–173. https://doi.org/10.4271/2017-01-0477

57. Rao HM, Kang J, Huff G, Avery K (2018) Impact of specimen configuration on fatigue properties of self-piercing riveted aluminum to carbon fiber reinforced polymer composite. Int J Fatigue 113:11–22. https://doi.org/10.1016/j.ijfatigue.2018.03.031

58. Di Franco G, Fratini L, Pasta A (2012) Influence of the distance between rivets in self-piercing riveting bonded joints made of carbon fiber panels and AA2024 blanks. Mater Des 35:342–349. https://doi.org/10.1016/j.matdes.2011.09.036

59. Liang J, Jiang H, Zhang J, Wu X, Zhang X, Li G, Cui J (2019) Investigations on mechanical properties and microtopography of electromagnetic self-piercing riveted joints with carbon fiber reinforced plastics/aluminum alloy 5052. Arch Civ Mech Eng 19:240–250. https://doi.org/10.1016/j.acme.2018.11.001

60. Kang J, Rao H, Zhang R, Avery K, Su X (2016) Tensile and fatigue behaviour of self-piercing rivets of CFRP to aluminium for automotive application. IOP Conf Ser Mater Sci Eng 137:12025. https://doi.org/10.1088/1757-899X/137/1/012025

61. Meschut G, Gude M, Augenthaler F, Geske V (2014) Evaluation of damage to carbon-fibre composites induced by self-pierce riveting. Procedia CIRP 18:186–191. https://doi.org/10.1016/j.procir.2014.06.129

62. Fratini L, Ruisi VF (2009) Self-piercing riveting for aluminium alloys-composites hybrid joints. Int J Adv Manuf Technol 43:61–66. https://doi.org/10.1007/s00170-008-1690-3

63. Xue Z, Wang X, Xu C, Chen Z, Feng Q, Liu J, Li L (2023) Equivalent characterization of pre-strained material properties and mechanical behavior prediction of steel/aluminum self-piercing riveted joints. Thin-Walled Struct 182:110243. https://doi.org/10.1016/j.tws.2022.110243

64. Leconte N, Bourel B, Lauro F, Badulescu C, Markiewicz E (2020) Strength and failure of an aluminum/PA66 self-piercing riveted assembly at low and moderate loading rates: experiments and modeling. Int J Impact Eng 142:103587. https://doi.org/10.1016/j.ijimpeng.2020.103587

65. Arcan M, Hashin Z, Voloshin A (1978) A method to produce uniform plane-stress states with applications to fiber-reinforced materials - a specially designed specimen yields material properties under pure shear or uniform plane-stress conditions. Exp Mech 18:141–146. https://doi.org/10.1007/BF02324146

66. Karim MA, Bae J-H, Kam D-H, Kim C, Park Y-D (2019) Critical influence of rivet head height on corrosion performance of CFRP/aluminum self-piercing riveted joints. Corros Sci Technol 118:92–101. https://doi.org/10.14773/cst.2019.18.3.92

67. Jiang H, Sun L, Dong D, Li G, Cui J (2019) Microstructure and mechanical property evolution of CFRP/Al electromagnetic riveted lap joint in a severe condition. Eng Struct 180:181–191. https://doi.org/10.1016/j.engstruct.2018.11.042

68. Lim YC, Jun J, Leonard DN, Li Y, Chen J, Brady MP, Feng Z (2021) Study of galvanic corrosion and mechanical joint properties of AZ31B and carbon-fiber–reinforced polymer joined by friction self-piercing riveting. J Magnes Alloy. https://doi.org/10.1016/j.jma.2021.05.003

69. Mandel M, Krüger L (2013) Determination of pitting sensitivity of the aluminium alloy EN AW-6060-T6 in a carbon-fibre reinforced plastic/aluminium rivet joint by finite element simulation of the galvanic corrosion process. Corros Sci 73:172–180. https://doi.org/10.1016/j.corsci.2013.03.033

70. Mandel M, Krüger L (2015) Long-term corrosion studies of a CFRP/EN AW-6060-T6 self-piercing rivet joint and a steel/EN AW-6060-T6 blind rivet joint. Mater Today Proc 2:S131–S140. https://doi.org/10.1016/j.matpr.2015.05.030

71. Karim MA, Bae J-H, Kam D-H, Kim C, Choi W-H, Park Y-D (2020) Assessment of rivet coating corrosion effect on strength degradation of CFRP/aluminum self-piercing riveted joints. Surf Coatings Technol 393:125726. https://doi.org/10.1016/j.surfcoat.2020.125726

72. Available at: https://www.youtube.com/watch?v=o7Co5cZhOUw. Accessed 4 May 2020

73. Available at: https://www.dynaexamples.com/introduction/process_simulation/self-piercing-riveting. Accessed 27 Feb 2023

74. Bouchard PO, Laurent T, Tollier L (2008) Numerical modeling of self-pierce riveting—From riveting process modeling down to structural analysis. J Mater Process Technol 202:290–300. https://doi.org/10.1016/j.jmatprotec.2007.08.077

75. Available at: https://www.simufact.com/module-mechanical-joining.html. Accessed 2 Nov 2023.

76. Atzeni E, Ippolito R, Settineri L (2007) FEM Modeling of Self-Piercing Riveted Joint. Key Eng Mater 344:655–662. https://doi.org/10.4028/www.scientific.net/KEM.344.655

77. Casalino G, Rotondo A, Ludovico A (2008) On the numerical modelling of the multiphysics self piercing riveting process based on the finite element technique. Adv Eng Softw 39:787–795. https://doi.org/10.1016/j.advengsoft.2007.12.002

78. Puck A, Schürmann H (1998) Failure analysis of frp laminates by means of physically based phenomenological models. Compos Sci Technol 58:1045–1067. https://doi.org/10.1016/S0266-3538(96)00140-6

79. Drossel WG, Mauermann R, Grützner R, Mattheß D (2013) Numerical and experimental analysis of self piercing riveting process with carbon fiber-reinforced plastic and aluminium sheets. Key Eng Mater 554–557:1045–1054. https://doi.org/10.4028/www.scientific.net/KEM.554-557.1045

80. Rao Z, Ou L, Wang Y, Wang P-C (2020) A self-piercing-through riveting method for joining of discontinuous carbon fiber reinforced nylon 6 composite. Compos Struct 237:111841. https://doi.org/10.1016/j.compstruct.2019.111841